

See discussions, stats, and author profiles for this publication at: <https://www.researchgate.net/publication/394430558>

# Addressing Practical Challenges of Stochastic Process Control for Leakage Detection in Water Distribution Networks: A Comparative Analysis

Article in Journal of Water Resources Planning and Management · August 2025

DOI: 10.1061/JWRMD5.WRENG-6969

---

CITATIONS

0

READS

80

2 authors:



Ella Steins

Technische Universität Berlin

7 PUBLICATIONS 9 CITATIONS

[SEE PROFILE](#)



Andrea Cominola

Technische Universität Berlin

71 PUBLICATIONS 1,826 CITATIONS

[SEE PROFILE](#)

<sup>1</sup> Addressing practical challenges of stochastic process control for leakage  
<sup>2</sup> detection in water distribution networks: a comparative analysis

<sup>3</sup> Ella Steins\* and Andrea Cominola †

<sup>4</sup> **Abstract**

<sup>5</sup> Various leakage detection algorithms have been proposed in the literature to pursue  
<sup>6</sup> prompt leakage identification in water distribution networks using sensor data. Some use  
<sup>7</sup> stochastic process control (SPC) methods, where the leak identification is considered an  
<sup>8</sup> anomaly detection problem. However, several practical challenges emerge from SPC in leakage  
<sup>9</sup> detection, including outliers, random fluctuations, as well as non-normally distributed and  
<sup>10</sup> autocorrelated data. Here, we contribute a comparative analysis of seven advanced SPC  
<sup>11</sup> techniques based on cumulative sum (CUSUM) for leakage identification in water distribution  
<sup>12</sup> networks, selected based on an extensive literature review of approximately 100 publications.  
<sup>13</sup> We test their usability for leakage detection by integrating them into a state-of-the-art  
<sup>14</sup> data-driven detection method and demonstrating them on the L-Town benchmark network.  
<sup>15</sup> Ultimately, this study offers actionable recommendations to guide the selection of change point  
<sup>16</sup> detection methods for leakage detection: our results indicate that transformations are best  
<sup>17</sup> combined with robust statistics. Nonparametric and adaptive methods are suited to retrieve  
<sup>18</sup> reliable alarms under heterogeneous conditions. Lastly, incorporating a decorrelation step  
<sup>19</sup> improves the detection performance if irregular water demand patterns occur in the network.

---

\*Postdoc, Chair of Smart Water Networks, Technische Universität Berlin, Berlin 10623, Germany; Einstein Center Digital Future, Berlin 10117, Germany (corresponding author). ORCID: <https://orcid.org/0000-0002-1615-494X>. Email: steins@tu-berlin.de

†Assistant Professor, Chair of Smart Water Networks, Technische Universität Berlin, Berlin 10623, Germany; Einstein Center Digital Future, Berlin 10117, Germany. ORCID: <https://orcid.org/0000-0002-4031-4704>. Email: andrea.cominola@tu-berlin.de

20        **Keywords**— Leakage detection, stochastic process control, CUSUM, GWMA-CUSUM, weighted  
21        CUSUM, robust statistics, nonparametric & adaptive control charts, autocorrelation, water distribution  
22        network

23        

## 1 Introduction

24        Water scarcity is expected to dramatically increase by 2050 due to growing demand, **increasing** pollution of  
25        **freshwater sources, and the declining** availability of water resources (Boretti and Rosa 2019). Along with  
26        infrastructure aging, these represent major challenges to water distribution networks (WDNs) management,  
27        where the amount of non-revenue water is already estimated to be 126 billion cubic meters per year  
28        worldwide (Liemberger and Wyatt 2019). A substantial part of non-revenue water is due to leakages  
29        (Bozkurt et al. 2022), which, **beyond the direct economic damage due to the revenue loss**, also lead to  
30        cascading **economic** costs due to, e.g., increased operational energy consumption (Liemberger and Marin  
31        2006), as well as to potential public health risk through water contamination (LeChevallier et al. 2003;  
32        Fox et al. 2016). Addressing these critical issues reinforces the need for proper **solutions** to detect and  
33        mitigate leaks in WDNs, ensuring more sustainable and resilient water **supply**.

34        Considerable research has been conducted in the last decades to advance leakage management by  
35        developing various leakage identification and localization methods (Puust et al. 2010). Leak identification  
36        **aims to detect** a leakage occurrence promptly, i.e., with the lowest time to detection (TTD), defined as the  
37        difference between its detection time and its start time. Leak localization, in turn, deals with **determining**  
38        the leak position in a WDN. Unlike hardware-based methods, software-based methods enable real-time  
39        monitoring of changes in flow and pressure regimes by processing observations from a WDN (Wan et al.  
40        2022). They can be categorized into model-based, mixed data-driven and model-based (also known as  
41        hybrid), and data-driven methods (Romero-Ben et al. 2023). Model-based methods require a calibrated  
42        hydraulic model of the WDN. While these models are well suited to capture the system topology, **its**  
43        hydraulic processes, and operations, **their selection and applicability are restricted due to calibration**  
44        **difficulties arising from the complexity of WDNs (Kim et al. 2016)** as well as **uncertainties in the considered**  
45        **system parameters (Blesa and Pérez 2018)**. Mixed approaches aim to circumvent these problems by  
46        limiting the usage of hydraulic models to offline processes and combining them with data-driven techniques,  
47        including machine learning. Lastly, **data-driven** methods abstain from sophisticated **hydraulic models**.  
48        Further differentiated into unsupervised, semi-supervised, and supervised methods (Wu et al. 2024), **they**

49 directly process WDN flow or pressure measurements (unsupervised), employ prediction-classification  
50 techniques or reconstruction error analysis (semi-supervised), or develop supervised classification trained  
51 with labeled data. Hence, data-driven methods do not face the requirements needed for calibration of  
52 model-based approaches, yet supervised and semi-supervised methods still require training data, and their  
53 performance typically depends on the availability and quality of such data (Mounce and Machell 2006).  
54 Hence, the requirements of leakage detection and identification methods are not mutually exclusive.

55 In this work, we focus on statistical process control (SPC) techniques, which are commonly employed  
56 by both unsupervised and semi-supervised data-driven methods. SPC techniques use statistics to detect  
57 the change point of a process, where it is crucial to differentiate random changes from actual change points  
58 (Ali et al. 2016), i.e., points in a time series or data sequence at which the underlying statistical properties  
59 undergo a significant shift. In an SPC perspective, the leakage detection problem is regarded as an anomaly  
60 detection problem, which has also been described as “the problem of finding patterns in data that do not  
61 conform to expected behavior” (Chandola et al. 2009). Based on an estimation of the statistical moments,  
62 threshold boundaries are constructed from historical data (direct measurements or reconstruction error  
63 time series) and used to distinguish between anomalies (i.e., leakage) and normal observations. For the  
64 purpose of leakage identification, various SPC techniques have been employed, including straightforward  
65 thresholding, Shewart control charts and Western Electric Control rules (Bakker, Vreeburg, et al. 2014;  
66 Romano et al. 2017; Farah and Shahrour 2017; Wang et al. 2020; Bakker, Jung, et al. 2014; Kim et al.  
67 2016; Wu, Peng, et al. 2023; Loureiro et al. 2016; Romano et al. 2014), univariate exponentially weighted  
68 moving average (EWMA), univariate cumulative sum (CUSUM) control charts (Daniel, Pesantez, et al.  
69 2022; Steffelbauer et al. 2022; Eliades and Polycarpou 2012; Anjana et al. 2015; Ahn and Jung 2019;  
70 Jung, Kang, et al. 2015; Jung and Lansey 2015; Misiunas et al. 2006), and multivariate control charts and  
71 Hotelling’s  $T^2$  (Jung, Kang, et al. 2015; Jung and Lansey 2015; Palau et al. 2012). While SPC methods are  
72 overall computationally efficient and do not require a comparable amount of training data to supervised  
73 methods, they may be built on unrealistic assumptions (Wan et al. 2022).

74 Three main practical challenges emerge from the existing integration of SPC methods in leakage  
75 detection algorithms – first, data fluctuations. In a comparative analysis of SPC methods, Jung and Lansey  
76 (2015) compared different univariate and multivariate methods and found the univariate CUSUM and  
77 EWMA charts to be less sensitive to outliers in the data than multivariate methods. However, they are  
78 more sensitive to small leaks (Jung and Lansey 2015). Additionally, they discussed that the control charts

79 rely on the assumption that all data is uncorrelated and comes from the same distribution, which might  
80 not hold due to daily fluctuations in the flow. To address this limitation, Palau et al. (2012) proposed  
81 to divide the day into different periods due to daily fluctuations in the flow and perform a principal  
82 component analysis to further reduce variability. Cumulative integrals of shifted pressure data (Kim et al.  
83 2016), moving averages (Bakker, Vreeburg, et al. 2014; Bakker, Jung, et al. 2014), or moving standard  
84 deviations (Farah and Shahrour 2017) are suggested to denoise and smooth variations. Additionally, input  
85 variables are often normalized to remove fluctuations (Ahn and Jung 2019).

86 A second common problem resides in setting the threshold that enables discriminating between  
87 anomalous and normal observations (Wang et al. 2020; Kim et al. 2016; Wu, Peng, et al. 2023; Eliades  
88 and Polycarpou 2012; Nimri et al. 2023; Soldevila, Blesa, et al. 2016). While a lower threshold improves  
89 the detection of small leaks, it might also cause false alarm reporting, i.e., an increase in false positive  
90 (FP) rate. Some methods mitigate this issue by employing multiple control charts with varying thresholds  
91 (Wang et al. 2020; Bakker, Jung, et al. 2014) or choosing thresholds based on computed statistics for  
92 small leaks in historical data sets (Eliades and Polycarpou 2012). Further, an outlier detection or leakage  
93 verification step before or after the respective leak detection step is often proposed in the literature (Bakker,  
94 Vreeburg, et al. 2014; Wang et al. 2020; Soldevila, Boracchi, et al. 2022) to reduce the effect of outliers  
95 caused by sensor drifts, errors, or other anomalies not attributed to leaks.

96 Finally, most SPC methods assume normally distributed data. While this is rarely the practical case,  
97 little work in leakage detection addresses this problem. Buchberger and Nadimpalli (2004) propose a  
98 Box-Cox Transformation before comparing the trajectories of the observations to the standard normal plot,  
99 and Loureiro et al. (2016) introduce a correction factor for heavy-tailed distributions to the Shewart chart.

100 In this paper, we address the above practical challenges of SPC methods for leakage detection by  
101 systematically and comparatively testing advanced SPC methods for data-driven leakage detection. We  
102 select seven representative state-of-the-art CUSUM-based methods, which have been developed in SPC  
103 literature over the last decades but have not yet been utilized for leakage detection problems. We selected  
104 them based on their potential to address the above-mentioned problems, where we explain the selection  
105 procedure in Section 3. This paper presents a novel methodological contribution to leak detection by  
106 systematically comparing the set of selected advanced SPC techniques against a set of practical limitations  
107 identified from extensive literature, thus offering both theoretical insight and directions for practical  
108 use. We integrate the selected CUSUM-based methods as the SPC step for leak identification into LILA

109 (leakage identification and localization algorithm), a recent state-of-the-art pressure-based algorithm  
110 for data-driven leakage identification and model-based localization (Daniel, Pesantez, et al. 2022). In  
111 its original version, LILA includes the standard CUSUM method (Page 1954) for leak identification.  
112 By demonstrating different SPC methods in combination with LILA, we ultimately aim at improving  
113 the overall usability of SPC methods for leakage detection and formulate technical recommendations  
114 concerning the following crucial capabilities: (i) avoid requiring historical leakage-free data, (ii) handle  
115 outliers, fluctuations, and non-normal data, (iii) increase sensitivity to small and non-constant changes  
116 (e.g., small transient leaks), and (iv) reduce the need for heuristic hyperparameter setting. In short, the  
117 tested methods include techniques such as weighting and an EWMA-CUSUM combination of the data  
118 points to increase sensitivity towards incipient leaks, transformations to approximate normal distributions,  
119 robust statistics to handle outliers, nonparametric methods that drop assumptions on the underlying data  
120 distribution, adaptive features to detect variable ranges of changes, self-starting schemes to avoid the need  
121 of historical data, and decorrelation to limit the influence of fluctuations.

122 The remainder of this paper is structured as follows: first, we introduce the L-Town network used as a  
123 case study in this work and LILA in Section 2. The L-Town network is a benchmark problem for testing  
124 leakage detection and localization methods, developed as part of the Battle of Leakage Detection and  
125 Isolation Methods (BattLeDim) (Vrachimis et al. 2022). The problems of the original CUSUM method are  
126 discussed using the example of employing it within LILA for the benchmark problem, as done in Daniel,  
127 Pesantez, et al. (2022). We then present the selected advanced CUSUM methods in Section 3. Within the  
128 framework of LILA, these methods are tested on the L-Town WDN and the numerical results are presented  
129 in Section 4. For each advanced CUSUM method, standard metrics for leakage identification are quantified,  
130 i.e., average time to detection (aTTD), precision, recall, and the  $F_1$ -score. Based on these metrics, the  
131 methods are compared in Section 5, including discussion of their respective use-cases, hyperparameter  
132 settings, and transferability. Lastly, Section 6 intends to offer a takeaway for including SPC methods  
133 in the future development of leakage detection and localization methods. Tables with the nomenclature  
134 (Table 7) and abbreviations (Table 8) used within this paper are reported in the Appendix (Section A.4).

## 135 2 Current limitations of the standard CUSUM

136 In this work, we identify the major challenges related to the usage of CUSUM-based SPC methods for  
137 leak detection by considering the demonstrative case study of the L-Town WDN (Vrachimis et al. 2022)

138 and LILA for leak identification (Daniel, Pesantez, et al. 2022).

139 The L-Town benchmark WDN, based on an actual WDN in Cyprus, was introduced as part of  
140 the BattLeDim competition to enable objective comparative performance evaluation of methods for the  
141 detection and localization of leakage events (see all details in Vrachimis et al. 2022). L-Town is characterized  
142 by a total length of 42.6 km with 785 nodes, 905 pipes, one pump, three valves, two reservoirs, and one  
143 tank. It consists of three district meter areas (DMAs). While DMAs A and B are each connected to a  
144 reservoir, a tank that refills during night is used to supply DMA C. A total of 33 pressure sensors, 82  
145 advanced meter reading (AMR) devices within DMA C, and flow meters at the outlet of each reservoir  
146 report data through a Supervisory Control and Data Acquisition (SCADA) system every five minutes.  
147 We here focus on the data collected in year 2019, which include a total of 19 leakages (8 abrupt and 11  
148 incipient leakages). Figure 1 shows the layout of the L-Town network with the three DMAs and positions  
149 of the 19 leakages. Their respective locations (pipe ID), start time and end time are given in Table 1. If a  
150 leak remained unfixed throughout the year 2019, the end time is set to 2019-12-31 23:55.

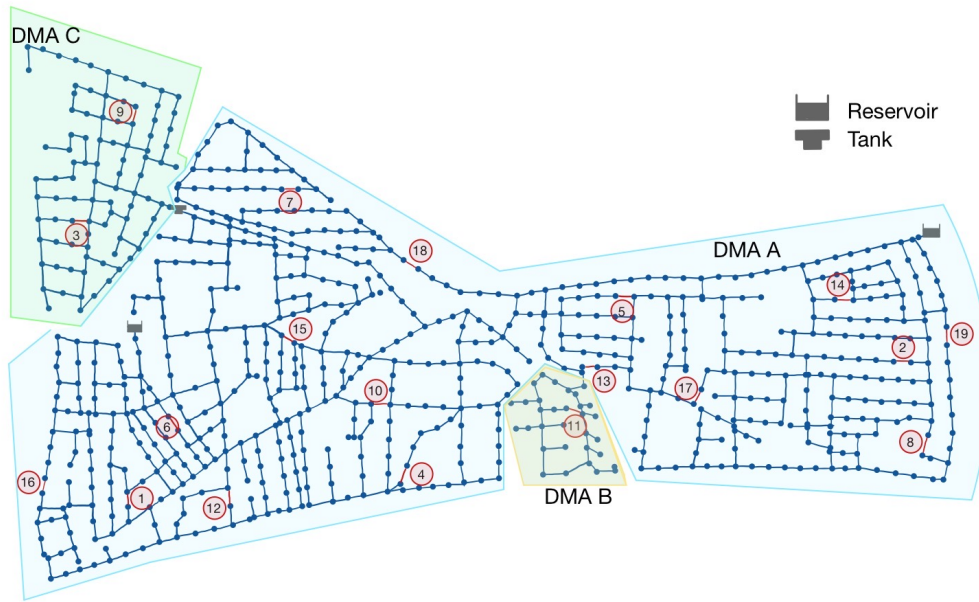


Figure 1: Layout of the L-Town WDN with three DMAs A, B, and C, and the 19 leakages that start during 2019. Figure adapted from Vrachimis et al. (2022).

151 While different approaches and methods for leak detection and identification have been developed  
152 and tested on L-Town as part of the BattLeDIM, data-driven methods are especially valuable for leakage  
153 identification and, possibly, localisation if a hydraulic model is not available. Here, we limit the scope of

Table 1: Overview of leaks in BattLeDIM data set

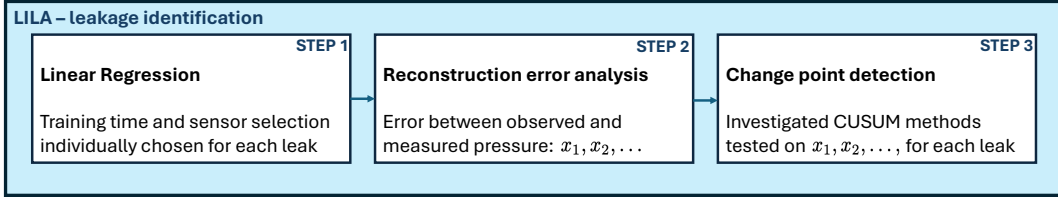
leak ID	pipe ID	start time	end time
1	<i>p523</i>	2019-01-15 23:00	2019-02-01 09:50
2	<i>p827</i>	2019-01-24 18:30	2019-02-07 09:05
3	<i>p280</i>	2019-02-10 13:05	2019-12-31 23:55
4	<i>p653</i>	2019-03-03 13:10	2019-05-05 12:10
5	<i>p710</i>	2019-03-24 14:15	2019-12-31 23:55
6	<i>p514</i>	2019-04-02 20:40	2019-05-23 14:55
7	<i>p331</i>	2019-04-20 10:10	2019-12-31 23:55
8	<i>p193</i>	2019-05-19 10:40	2019-12-31 23:55
9	<i>p277</i>	2019-05-30 21:55	2019-21-31 23:55
10	<i>p142</i>	2019-06-12 19:55	2019-07-17 09:25

leak ID	pipe ID	start time	end time
11	<i>p680</i>	2019-07-10 08:45	2019-12-31 23:55
12	<i>p586</i>	2019-07-26 14:40	2019-09-16 03:20
13	<i>p721</i>	2019-08-02 03:00	2019-21-31 23:55
14	<i>p800</i>	2019-08-16 14:00	2019-12-31 23:55
15	<i>p123</i>	2019-09-13 20:05	2019-21-31 23:55
16	<i>p455</i>	2019-10-03 14:00	2019-12-31 23:55
17	<i>p762</i>	2019-10-09 10:15	2019-12-31 23:55
18	<i>p426</i>	2019-10-25 13:25	2019-12-31 23:55
19	<i>p827</i>	2019-11-20 11:55	2019-12-31 23:55

our study on the leakage identification step only, and consider the semi-supervised data-driven method LILA proposed by Daniel, Pesantez, et al. (2022) to demonstrate and discuss SPC techniques for leakage detection. As the leak identification module in LILA is data-driven, it does not require a calibrated hydraulic model of the WDN. The leak identification module of LILA, described in detail in Daniel, Pesantez, et al. (2022), consists of the three steps represented in Figure 2: LILA first estimates pressure values at each time step at all WDN nodes by a linear prediction model, which makes use of the Bernoulli equation to formulate a linear regression between node pairs. This relationship is trained on time series of pressure data referred to normal WDN operations. The published version of LILA does not automate the selection of training periods and sensor selections, which are instead individually chosen for each leak in the published code (Daniel et al. 2021). While this represents a limitation of the published LILA, we consider the same training periods and sensor selection (Daniel et al. 2021) in this work to allow for consistent comparison with the published results. After training of the prediction model, a model reconstruction analysis compares the regression estimates with pressure data. Here, the error between estimated and observed pressure values, i.e., the model reconstruction error (MRE), is computed at each node. At last, LILA performs a change point detection step. It uses the CUSUM control chart to analyze the time series of the MRE (hereafter indicated with  $x_1, x_2, \dots$ , where the subscript index refers to the time index, retrieving the starting time of a potential leakage. In this work, we modify this step of LILA (step 3 in Figure 2) by injecting the selected CUSUM-based methods for comparative performance analysis. Hence, the selected methods are tested on the error time series of the 19 leaks in the BattLeDIM data set.

The CUSUM method implemented in the last step of the leak identification module in LILA (Daniel, Pesantez, et al. 2022) was originally introduced by Page in 1954 (Page 1954), and is referred to as the “standard” CUSUM control chart in the following. Let us consider a time series  $x$  representing the MRE of



*Figure 2: This flowcharts summarizes how the CUSUM methods are tested within LILA. The first two steps of the algorithm, namely the linear regression (step 1) and reconstruction error analysis (step 2), are performed once, resulting in an error time series  $x_1, x_2, \dots$ , for each leak. Here, the linear regression is carried out based on leak-wise individual training times and sensor selection, taken from Daniel et al. (2021). In the last step, a change point detection is performed, where the standard CUSUM method is used in the published version of LILA (Daniel, Pesantez, et al. 2022). The selected CUSUM-based methods are integrated in this step by testing them on the error time series  $x_1, x_2, \dots$ , of each respective leak in the 2019 BattLeDIM data set.*

176 a selected sensor node. The positive cumulative sum  $C_i^+$  can be calculated at time step (iteration)  $i \geq 1$   
 177 as follows:

$$C_i^+ = \max [0, x_i - (\mu_0 + K) + C_{i-1}^+], \quad (1)$$

178 for given mean  $\mu_0$ , slack value  $K$ , and  $C_0^+ = 0$ . An alarm is raised if the distance from the target variable  
 179 exceeds a predefined threshold  $H > 0$ , i.e.,  $C_i^+ > H$ . In the context of leak detection, only the positive  
 180 cumulative sum of the distance is computed, as leaks lead to pressure drops and, subsequently, to an  
 181 increase in the MRE time series. The standard CUSUM method is a repetitious application of Wald's  
 182 Sequential Probability Test (Wald 1945) with chosen initial score and control bounds (Polunchenko 2016),  
 183 by testing if the probability density function (pdf) of a series of independent observations  $x_1, x_2, \dots$  has  
 184 changed from  $f_0(x)$  (the in-control distribution) to  $f_1(x) \neq f_0(x)$  (the out-of-control distribution). For the  
 185 test,  $f_0$  and  $f_1$  are assumed to be known and normally distributed, where  $f_0 = \mathcal{N}(\mu_0, \sigma_0)$ .

186 In practice, the mean and standard deviation, as well as the hyperparameters needed to set the values  
 187 of  $K$  and  $H$  are estimated using an in-control data set. This step is referred to as Phase I, while Phase II  
 188 refers to monitoring the process to detect changes (Jones-Farmer et al. 2009). Typically, the slack value  
 189  $K$  and the threshold  $H$  are set to be multipliers of the standard deviation of the in-control data, i.e.,  
 190  $K = k \cdot \sigma_0$  and  $H = h \cdot \sigma_0$ . These formulations require setting hyperparameters  $k$  and  $h$ . A common  
 191 approach is setting  $k = \frac{\delta}{2}$ , where  $\delta$  is based on the mean shift magnitude  $\delta = \mu_1 - \mu_0$  that is to be detected  
 192 (Moustakides 1986), and either selecting an adequate threshold  $H$  based on metrics of the in-control data  
 193 set or empirical knowledge.

194 The assumptions required by the standard CUSUM method, however, do not hold true for many

real-world leakage detection cases. More specifically, three limitations may hamper the usage of the standard CUSUM method within data-driven or mixed algorithms such as LILA. The following challenges become particularly evident when using LILA with standard CUSUM on the L-Town WDN benchmark (please note that the test statistics and histograms of the respective leaks mentioned below are shown in Appendix A.3):

**1. Known and normally-distributed in-control distribution:** the mean and variance of the variable observed for SPC are usually approximated based on an available set of in-control samples. This set might be too small for accurate approximations or might even be not available at all, limiting the informed setting of the slack and threshold values. In Daniel, Pesantez, et al. (2022), the standard CUSUM method computes the mean and variance of the in-control distribution based on the first three days of observations, for instance. However, leak 16 of the benchmark problem starts within 48 hours of the sampled data (Vrachimis et al. 2022). The in-control set needed for the CUSUM methods differentiate from the training set needed for the linear regression in LILA (step 1 in Figure 2), as the in-control set is selected at the beginning of the error time series which is retrieved after the linear regression. Hence, SPC methods that avoid historical data can still be preferable to those that need an in-control set. Further, outliers can affect the performance of the standard CUSUM method, and noise levels vary between the controlled MRE time series. Lastly, the MRE might not be normally distributed at all. The assumption of normally-distributed values limits the applicability of the method to the case of pressure estimates without systematic errors. This limitation is particularly relevant considering that LILA is intended to be used in scenarios in which not all system properties are known. For the benchmark test, for instance, leak 3 and leak 9 lie in a DMA with unknown irregular demands. Consequently, the respective MRE time series do not exhibit normal behavior. In Daniel, Pesantez, et al. (2022), customized CUSUM parameter settings ( $k = 0.5$  and  $h = 300$ ) were adopted *ad hoc* for these leaks, as the threshold and slack parameter values used for all other time series ( $k = 2$  and  $h = 3$ ) would lead to false alarms in both cases. Additionally, the set of in-control samples was extended to 14 days for approximating the values of mean and variance. This showcases the difficulty of finding suitable global parameters across all MRE time series with the standard CUSUM method. Based on the Kolmogorov-Smirnov test for normality (Massey 1951), leaks 1, 6, 13, and 18 also show non-normal in-control distributions.

**2. Known mean change:** the standard CUSUM method selects the slack parameter based on a fixed mean change that is to be detected. However, in practice, the magnitude of the mean change may

vary substantially due to different leak sizes. Additionally, incipient leaks do not cause an abrupt change in the mean of the MRE. The  $h$  threshold would need to be reduced to shorten the TTD for these leaks. However, a smaller threshold would result in an increase of the overall FP rate, if this threshold was chosen globally for all time series. This further limits the selection of an adequate and generalizable threshold.

**3. Autocorrelation:** while the standard CUSUM assumes independent observations, some MRE time series are autocorrelated due to the hydraulic of the physical WDN. Again, this is possibly the case, if the forecast model does not account for all actual demands. Based on the Durbin-Watson statistic (Durbin and Watson 1992) of the in-control data, this is indeed the case for four out of 19 leakages in the BattLeDIM benchmark dataset (leaks 3,5,9, and 11). The corresponding test statistics are shown in Appendix A.3.

### 3 CUSUM-based method selection for comparative analysis

The practical challenges of the standard CUSUM within LILA identified above - i.e., outliers and random variations, non-normal in-control distributions, variable leak size, sensitivity towards small & incipient leaks, and autocorrelation of the data - demonstrate with a specific example the main broader challenges of SPC methods for leakage identification in literature as described in the Introduction: data fluctuations can be either caused by outliers & random variations, and irregular patterns or autocorrelated data might even lead to significantly non-normal distributions. Furthermore, the detection of small & incipient leaks with standrad SPC techniques requires a small threshold; however, finding a suitable threshold is then challenging due to variable & priorly unknown leak sizes.

To address these challenges, we test seven methods. They are summarized in Table 2, along with a short description of their main features and capabilities and literature references. Our selection is based on an extensive literature review of approximately 100 CUSUM (and other SPC) publications. While the full literature review is omitted here as it is not within the primary scope of this paper, and reference is made to other recent comprehensive reviews of SPC methods (Yu and Cheng 2022; Granjon 2013; Saleh et al. 2023; Montgomery 2019), we summarize here our selection procedure and rationale. We primarily limit the approach to univariate CUSUM-based methods, as its challenges are representative for SPC methods in general, and comparison to the standard univariate CUSUM employed in LILA is straightforward. Further, EWMA and CUSUM methods have been previously found superior to other SPC methods for leakage identification (Jung, Kang, et al. 2015), and SPC methods are often used in combination. In particular,

combined EWMA and CUSUM charts are found to be more sensitive towards small shifts than other advanced methods (Lu 2017), and as such a combined chart is employed in this comparison as well (method  $gw$ ). First, we select four SPC methods that address at least one of the identified challenges (methods  $t$ ,  $tr$ ,  $w$ ,  $gw$  in Table 2). Then, three methods that address multiple challenges are subsequently tested (methods  $adn$ ,  $ac$ ,  $corr$  in Table 2). The seven methods can be grouped in three main classes, depending on the main challenge they address (non-normal distributions & data fluctuations, sensitivity towards smaller leaks, combinations of multiple challenges). Their rationale and assumptions are described in the following.

*Table 2: Summary of the selected CUSUM-based SPC methods for comparative analysis on leak detection.*

Acronym	SPC method name	Main features
$t$	transformed CUSUM (Figueiredo and Gomes 2003)	approximate normality by transforming the data
$tr$	transformed & robust CUSUM (Figueiredo and Gomes 2003; Nazir et al. 2013)	approximate normality by transforming the data, increase robustness towards outliers by using the trimean
$w$	weighted CUSUM (Shu et al. 2008)	increase sensitivity by strong weighting of more recent data points, detection of non-constant changes in restricted time window
$gw$	GWMA-CUSUM (Lu 2017)	increase sensitivity by combining EWMA and CUSUM, more flexible weighting due to design parameter
$adn$	nonparametric & adaptive CUSUM (Liu et al. 2014)	for any underlying distribution by using sequential ranks, for detecting a range of shifts by recursively estimating the expected mean shift, no in-control data: with self-starting scheme
$ac$	nonparametric & adaptive CUSUM for arbitrary change (Li 2021)	for any underlying distribution by using data categorization, for detecting a range of shifts by recursively estimating out-of-control distribution, no in-control data: self-starting scheme, for arbitrary change by using statistics for location and scale changes in parallel
$corr$	nonparametric & adaptive CUSUM for autocorrelated data (Liu et al. 2014; Li and Qiu 2020)	for any underlying distribution by using sequential ranks, for detecting a range of shifts by recursively estimating the expected mean shift, no in-control data: with self-starting scheme, for autocorrelated data by de-correlation using Cholesky decomposition

Table 3 summarizes the challenges which are addressed by the respective selected CUSUM-based SPC method. The column *increased sensitivity* refers to increased detection sensitivity towards small incipient leaks, either due to weights or consideration of scale changes. Adaptive techniques enable detection of *unknown shift magnitudes*. While robust methods increase the ability to handle *outliers*, fully *non-normal distributions* can be handled by either transformations or non-parametric formulations. Lastly, *autocorrelation* of the data is addressed by a decorrelation step. By use of adaptive and non-parametric statistics, self-starting schemes can be formulated that reduce or even remove the need of in-control data. Similarly, acknowledging both non-normality and autocorrelation reduces the need of heuristic hyperparameter settings due to random fluctuations.

First, to deal with the challenge of non-normal or unknown distributions, *transformations* of the data are generally implemented. While the z-score is commonly used to standardize data, the Box-Cox transformation and Yeo-Johnson can be used to approximate normality. However, the interpretability of

274 the transformed data might suffer and transformations might be inappropriate to use in case the underlying  
275 model exhibits systematic errors. Further, they do not tackle any of the other problems in question.  
276 Therefore, transformations are often proposed together with robust statistics with the goal of robustness  
277 towards outliers or noise. We here combine the Box-Cox transformation, z-score (Figueiredo and Gomes  
278 2003) ([method \*t\*](#)) and the use of a robust statistic (Nazir et al. 2013) ([method \*tr\*](#)).

279 Second, *weighted CUSUM methods* are commonly employed to attribute higher weights to recent data,  
280 thus improving the sensitivity of CUSUM to gradual changes. Gradual changes may be generated, in our  
281 case, by incipient leaks. More recently, mixed GWMA-CUSUM have been shown superior in detecting  
282 certain shifts than EWMA or CUSUM methods. Here we test a weighting method designed for fast  
283 detection of non-constant mean shifts ([method \*w\*](#)), as well as the GWMA-CUSUM scheme ([method \*gw\*](#)),  
284 specifically for their capabilities of detecting incipient leaks. However, both methods fall short in dealing  
285 with arbitrary underlying distributions and the setting of the hyperparameters has to be designed for a  
286 fixed leak size.

287 Finally, we test *nonparametric and adaptive methods* to treat both non-normality and the sensitivity  
288 towards small shifts: [adaptive](#) methods avoid setting the hyperparameters based on a fixed target mean  
289 shift by employing adaptive strategies. Nonparametric (also referred to as distribution-free) methods use  
290 nonparametric statistics like sequential ranks and data categorization to detect change points. Hence, they  
291 can handle unknown distributions without any assumption of normality. We first test the nonparametric,  
292 adaptive method proposed in [Liu et al. \(2014\)](#) ([method \*adn\*](#)). It relies on a self-starting scheme, i.e.,  
293 it does not require an in-control data set. Additionally, we implement the nonparametric and adaptive  
294 CUSUM for arbitrary changes from [\(Li 2021\)](#) ([method \*ac\*](#)). This scheme has similar characteristics to  
295 the previous, but additionally tests for scale changes, which are potentially more suitable for detection  
296 of incipient leakages. Both methods still build on the assumption of independent observations. The  
297 nonparametric and adaptive method *adn* is also combined with a decorrelation technique (Li and Qiu  
298 2020) to treat autocorrelated data ([method \*corr\*](#)).

Table 3: Challenges addressed by each selected CUSUM-based SPC method for comparative analysis on leak detection.

Method acronym	increased sensitivity	unknown shift magnitude	outliers	non-normal distribution	autocorrelated data
<i>t</i>				x	
<i>tr</i>			x	x	
<i>w</i>	x				
<i>gw</i>	x				
<i>adn</i>		x		x	
<i>ac</i>	x	x		x	
<i>corr</i>		x		x	x

## 299 4 Numerical results and SPC performance assessment

300 In the following subsections, all [seven](#) selected methods are described in detail, together with their respective  
 301 performance on the L-Town test case. We here make a note on the hyperparameter setting: [the](#) average  
 302 run length of the in-control distribution, short  $ARL_0$ , which refers to the average number of points until a  
 303 false alarm is given, is commonly used to tune the hyperparametrs of the respective methods and ensure  
 304 comparability of different control charts. However, using the  $ARL_0$  does not lead to usable results for the  
 305 leakage detection problem at hand due to violation of the assumptions needed, [as](#) [the](#) theoretical relation  
 306 between  $ARL_0$  and FP rate does not hold. An example for the standard CUSUM method is given in  
 307 Appendix A.2. Yet, it is still possible to find hyperparameter settings which lead to reasonable results.  
 308 To still ensure comparability, we select the optimal hyperparameters for each method based on a grid  
 309 search that finds the smallest overall TTD while avoiding FPs. This uses out-of-control data, which is only  
 310 available if historical leak data is present, corresponding to an empirical hyperparameter setting. As some  
 311 of the methods are in need of less assumptions, theoretical settings based on in-control metrics become  
 312 more feasible. This is discussed in Section 5.

313 The standard CUSUM method, reported in Section 2 [and considered here as the baseline method](#),  
 314 results in FP for both leaks 3 and 9 of the Benchmark problem ([global hyperparameters  \$h = 3\$  and  \$k = 2\$ ,](#)  
 315 [and an in-control data set of 3 days](#)). Individual TTD for each respective leak are listed in [Figure 3](#)  
 316 ([CUSUM](#)). [For each method, the chosen hyperparameter settings related to the presented results in Figure](#)  
 317 [3 are summarized in Table 9 in the Appendix](#).

<i>leak ID</i>	<b>CUSUM</b>	<b>method t</b>	<b>method tr</b>	<b>method w</b>	<b>method gw</b>	<b>method adn</b>	<b>method ac</b>	<b>method corr</b>
1	0 days 00:05	0 days 00:00	0 days 00:10	0 days 00:05	0 days 00:05	0 days 17:00	0 days 10:00	0 days 06:35
2	0 days 00:00	0 days 00:00	0 days 00:20	0 days 00:05	0 days 00:05	0 days 17:20	0 days 10:20	0 days 06:45
3	<b>FP</b>	<b>FP</b>	4 days 18:25	<b>FP</b>	4 days 20:30	4 days 23:35	6 days 08:55	5 days 06:45
4	9 days 06:30	21 days 05:15	15 days 19:30	21 days 14:30	16 days 00:15	17 days 10:55	16 days 23:20	15 days 18:45
5	0 days 02:00	0 days 02:05	0 days 02:45	0 days 04:25	0 days 03:35	0 days 14:05	0 days 17:25	1 days 15:15
6	0 days 00:10	0 days 00:30	0 days 00:40	0 days 09:20	0 days 01:00	0 days 19:40	0 days 19:45	0 days 07:10
7	0 days 00:00	0 days 00:00	0 days 00:15	0 days 00:05	0 days 00:15	0 days 22:50	0 days 08:45	0 days 07:00
8	28 days 02:45	<b>FN</b>	49 days 21:45	<b>FN</b>	54 days 13:15	57 days 01:10	49 days 09:20	53 days 19:50
9	<b>FP</b>	<b>FP</b>	<b>FP</b>	<b>FP</b>	17 days 13:45	38 days 11:30	46 days 01:40	59 days 23:40
10	0 days 00:00	0 days 00:00	0 days 00:35	0 days 00:50	0 days 00:30	0 days 17:15	0 days 08:50	0 days 06:45
11	0 days 01:05	0 days 14:05	0 days 08:45	0 days 01:05	1 days 17:15	0 days 18:40	1 days 06:35	0 days 14:00
12	11 days 08:00	14 days 19:10	12 days 17:15	17 days 16:50	11 days 23:00	13 days 18:45	14 days 07:20	11 days 19:55
13	11 days 10:00	30 days 08:25	26 days 05:45	32 days 13:25	20 days 05:55	25 days 22:35	21 days 01:40	19 days 17:05
14	4 days 20:30	5 days 18:15	4 days 20:50	6 days 20:10	4 days 08:00	5 days 05:55	4 days 23:20	4 days 06:10
15	40 days 14:05	51 days 13:20	40 days 14:15	62 days 01:05	50 days 22:15	46 days 02:00	44 days 18:30	43 days 05:40
16	31 days 04:05	40 days 20:30	23 days 10:25	42 days 03:20	31 days 08:15	34 days 04:40	30 days 19:20	30 days 11:30
17	16 days 03:15	19 days 01:40	16 days 04:25	19 days 04:00	16 days 06:00	17 days 01:30	16 days 17:00	16 days 06:55
18	0 days 00:15	0 days 00:45	0 days 00:25	0 days 10:45	0 days 01:00	0 days 16:45	0 days 13:50	0 days 05:28
19	1 days 20:15	15 days 02:30	13 days 22:10	18 days 02:45	12 days 20:30	10 days 17:25	10 days 06:50	9 days 01:20

*Figure 3: Time to detection (TTD) for the standard CUSUM, used as a baseline, and the seven selected SPC methods. Each method is assessed on the 19 leaks included in the BattLeDIM dataset for the L-Town WDN (Vrachimis et al. 2022). Cell color is proportional to the TTD (the darker the color, the longer the TTD). Labels FP and FN indicate the presence of false positive (i.e., false alarms) or false negative (i.e., missed leaks) occurrences.*

### 318 Transformed & robust CUSUM (t & tr)

319 To deal with non-normal distributed data, transformations have been suggested, e.g. (Figueiredo and Gomes  
 320 2003; Hamasha et al. 2022; Peterson 2021), including the Box-Cox and Yeo-Johnson transformation. While  
 321 the latter can be used on non-positive data, the Box-Cox transformation assumes positive observations,  
 322 which is achieved by adding a sufficiently large constant. After observing equivalent performance for both  
 323 transformation methods in preliminary tests, we here focus on the results using the Box-Cox transformation  
 324 with subsequent z-score standardization, and follow the approach suggested in (Figueiredo and Gomes  
 325 2003). The Box-Cox transformation of a variable  $x$  is given by

$$x^{BC} = \begin{cases} \log(x + c) & \text{if } \lambda = 0 \\ \frac{(x+c)^{\lambda}-1}{\lambda} & \text{else ,} \end{cases} \quad (2)$$

326 where  $x^{BC}$  is the resulting transformed variable and  $c$  is a constant. The variable  $\lambda$  is chosen such that  
 327  $x^{BC}$  follows a normal distribution. The minimization of the negative log-likelihood function is employed  
 328 as an optimizer for  $\lambda$ . Accordingly, an in-control data set is needed for the optimization, which is here  
 329 chosen to be 3 days (except for leak 16, where only the first day is used due to the leak starting on the  
 330 second day). Hence, the optimal value for  $\lambda$  depends on the in-control data. To increase the robustness

331 of the estimation of  $\lambda$ , we implement the Bootstrap-estimation approach suggested in [Figueiredo and](#)  
 332 [Gomes \(2003\)](#): the procedure consists of generating 5000 Bootstrap-subsets of size 100, each based on  
 333 the in-control data, optimizing  $\lambda$  for each subset using the negative log-likelihood, and lastly choosing  
 334 the mean of all estimates as the final value for  $\lambda$ . [More](#) details on the Bootstrap samples can be found in  
 335 [Figueiredo and Gomes \(2004\)](#). After fixing  $\lambda$ , the Box-Cox transformation is applied to the in-control  
 336 data, such that its mean  $\mu_{tr}$  and standard deviation  $\sigma_{tr}$  can be computed. During phase II, the Box-Cox  
 337 transformation is applied to every new observation  $x_i$ . Additionally, the transformed observation  $x_i^{BC}$  is  
 338 then standardized by applying the z-score, i.e.

$$z_i = \frac{x_i^{BC} - \mu_{tr}}{\sigma_{tr}}. \quad (3)$$

339 As long as no leak occurs, the Box-Cox-transformed and standardized MRE time series is supposed to be  
 340 standard normally distributed. For  $i \leq 1$ , the CUSUM statistic for the transformed CUSUM ([method t](#)) is  
 341 then formulated as

$$C_i^+ = \max [0, z_i - K + C_{i-1}^+], \quad (4)$$

342 where  $C_0^+ = 0$ .

343 As data transformation and standardization do not guarantee robust performance of control charts  
 344 against outliers, they are commonly employed in combination with robust statistics. These are less affected  
 345 by outliers than mean and standard deviation. In (Figueiredo and Gomes 2003), the robust statistics total  
 346 median and total range are used in a Stewart control chart after transformation and standarization of the  
 347 variable. In order to derive the combined effect of transformation and robust statistics, we here implement  
 348 the trimean TM for CUSUM, as proposed by (Nazir et al. 2013). The trimean is a weighted average of the  
 349 mean and two quartiles ( $Q_1$  and  $Q_3$ ) (Tukey 1977), formulated as

$$TM = \frac{Q_1 + 2Q_2 + Q_3}{4}. \quad (5)$$

350 During phase II, the trimean is iteratively computed based on a subset of 5 consecutive samples  
 351  $\{z_{i-4}, z_{i-3}, z_{i-2}, z_{i-1}, z_i\}$ , where the subgroup size corresponds to a tested size in (Nazir et al. 2013).  
 352 For  $i = 4, 9, 14, \dots$ , we define  $j = 1, 2, \dots$  and

$$C_j^+ = \max [0, TM_j - K + C_{j-1}^+], \quad (6)$$

353 where  $C_0^+ = 0$ . The slack value  $K = k \cdot \sigma_{TM}$  and threshold  $H = h \cdot \sigma_{TM}$  depend on the standard deviation  
 354 of the trimean data, which is estimated using the in-control set. This is summarized as **method tr**.

355 The original hyperparameter setting of  $k = 2$  and  $h = 3$  leads to false alarms 3,9,10, and 13 for the  
 356 transformed method, and to FP for leaks 3, 8, 9, 10, and 13. We present the results for  $k = 3$  and  $h = 3$   
 357 for both statistics in [Figure 3](#) (**method t** and **method tr**). This hyperparameter setting was optimal for  
 358 both methods. Method *tr* leads to overall comparatively better results than method *t*, as only one FP  
 359 remains, while all other leaks are detected. Interestingly, the transformed and robust method is able to  
 360 handle the MRE data of leak 3, which is not the case for the standard CUSUM and method *t*. Hence, the  
 361 robust statistics seem to have a greater effect than the transformation by itself. This is not surprising:  
 362 while transformations normalize the data based on the in-control group, they are still sensitive to outliers  
 363 that appear during phase II (monitoring). The latter are likely for leakage detection problems due to  
 364 fluctuations in the flow, as well as irregular demands and system operations. If these are not present in  
 365 the in-control group, their influence cannot be mitigated by transformations, while robust statistics also  
 366 have an effect during the monitoring phase.

## 367 Weighted CUSUM (**w**)

368 In many cases, the mean shift is not constant but varies over time. This can occur if residual charts are  
 369 employed to deal with autocorrelated processes, or if disturbances are compensated by continuous process  
 370 adjustments (Shu et al. 2008). A possible consequence is the so-called “forecast recovery”, which refers to  
 371 the fast diminishing of the effect of a mean change. Hence, the detection has to happen within a restricted  
 372 time window. Weighted charts achieve this by attributing higher weight on recent deviations, where a  
 373 weighting factor  $w_i$  is introduced to each increment of the CUSUM chart, i.e.,  $w_i(x_i - (\mu_0 + k))$ .

374 While the time window for detection is not generally assumed to be limited for leakage detection,  
 375 incipient leaks lead to non-constant mean shifts. Additionally, the magnitude of the change can be much  
 376 smaller compared to the case of pipe bursts. Here, we test a weighted CUSUM method (**method w**)  
 377 introduced by [Shu et al. \(2008\)](#) to increase the performance of the CUSUM chart for incipient leaks. The  
 378 standard CUSUM method is extended by a weight factor  $w_i$  associated to the  $i$ th observation of the time  
 379 series as

$$C_i^+ = \max(0, w_i(x_i - (\mu_0 + k)) + C_{i-1}^+), \quad (7a)$$

380 starting with  $C_0^+ = 0$ , and  $w_i = |W_i|$ , where

$$W_i = (1 - \alpha)W_{i-1} + \alpha x_i, W_0 = 0. \quad (7b)$$

381 For each time step,  $W_i$  is the EWMA-estimator for the mean, with weight hyperparameter  $\alpha \in [0, 1]$ . By  
 382 using the EWMA-estimator, more recent data points are given a higher weight, as the weights exponentially  
 383 decrease for previous samples. The factor  $w_i(x_i - (\mu_0 + k)) + C_{i-1}^+$  in the CUSUM chart then provides a  
 384 measure of correlation between  $x_i$  and the level of mean changes (Shu et al. 2008). Designing this chart  
 385 includes the setting of three hyperparameters, for which a sequential searching procedure is included in Shu  
 386 et al. (2008). Seeking a global hyperparameter setting for all 19 processes considered, the setting is derived  
 387 by minimizing the aTTD while avoiding FPs. An extensive grid search showed that no combination of  
 388 hyperparameter settings results in the detection of leak 8 while avoiding a FP for leak 11. Further, just  
 389 as for the standard CUSUM method, using the same hyperparameter settings for leaks 3 and 9 as for  
 390 all other leakages, leads to FPs in both cases. Hence, we choose a hyperparameter setting which does  
 391 not detect leak 8, and raises false alarms for leak 3 and 9. The overall TTD for all other leaks is then  
 392 minimized based on a second grid search, resulting in  $H = 3 \cdot \sigma_0$ ,  $K = 2 \cdot \sigma_0$ , and  $\alpha = 0.75$ . The results  
 393 are listed in Figure 3 (method w).

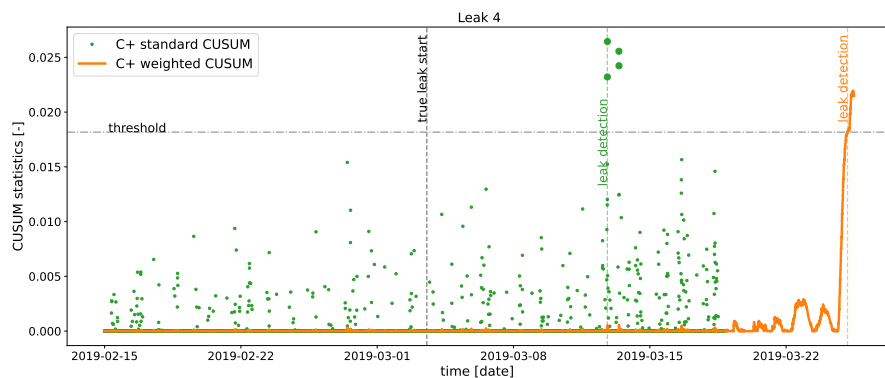


Figure 4: Standard vs. weighted CUSUM:  $C^+$  values are shown both for the standard CUSUM (green dots) and weighted CUSUM (orange line) for Leak 4.

394 The results show that the weighted method does not solve the problem of non-normal data with  
 395 high noise (leak 3 and 9). Further, the TTDs is not reduced for the incipient leaks. This is due to the  
 396 hyperparameter setting. If this was optimized for each respective time series, the corresponding TTDs  
 397 would be much shorter, in many cases less than a day. However, in order to be useful for the purpose

398 of leakage detection, an overall hyperparameter setting is desireable. Else, a tuning procedure would be  
399 needed on a large set of in-control data for each time series, and due to the violated relation between  
400  $ARL_0$  and the FP rate, the associated setting cannot guarantee a low FP rate. While the capability of  
401 the method for small incipient leaks might be underrepresented, this highlights the hyperparameter tuning  
402 as one of the crucial downsides. For example, while different value combinations of  $k$  and  $\alpha$  increase the  
403 capability of the method to detect multiple shift sizes, these combinations can only be found through  
404 empirical investigation.

405 On the other side, the method results in more reliable  $C^+$  statistics than the standard CUSUM. This  
406 is illustrated for example in leak 4 in Figure 4, which shows the respective  $C^+$  statistics over time for both  
407 the standard CUSUM and  $w$ . This type of Figure will be used throughout this work, as it gives insight  
408 into the fit of the respective methods for detecting the different leaks and dealing with the different error  
409 time series  $x_1, x_2, \dots$ , of the test study. In general, a flat  $C^+$  statistic close to zero before, and a steep and  
410 monotonically increasing  $C^+$  statistic after the true leak start show a reliable performance. In contrast,  
411  $C^+$ -values close to the threshold before the true leak start indicate an increased FP-risk for similar error  
412 time series. Further, the TTD is visualized by the horizontal distance between the true leak start and  
413 leak detection. In Figure 4, it can be seen that, while the hyperparameter setting of the weighted methods  
414 leads to rather late detection of the leak, it happens to a time for which the  $C^+$  statistic monotonically  
415 increases. This leads to a reliable performance regardless of the threshold setting. This is not true for the  
416  $C^+$  statistic of the standard method: Even though an alarm is raised pretty early, this is only due to four  
417 values, after which the statistic decreases again. Hence, the performance of the standard method is very  
418 sensitive to the selected threshold value. Additionally, the standard  $C^+$  statistic is close to the threshold  
419 before the true leak start, decreasing the reliable transferability to new detection problems of the standard  
420 CUSUM method.

## 421 GWMA-CUSUM ( $gw$ )

422 By proposing the GWMA-CUSUM chart, Lu (2017) combines two approaches to advance the detection  
423 of small shifts. The first approach lies in combinations of different charts. One example is the EWMA-  
424 CUSUM chart (Abbas et al. 2013), where the EWMA statistic is the input to the CUSUM chart, similar  
425 to the weighted CUSUM chart presented here (method  $w$ ). Additionally, certain shifts can be detected  
426 more effectively by introducing a more flexible weighting in the EWMA chart. GWMA charts achieve this

427 by introducing a design parameter  $q$  and adjustment parameter  $\tilde{\alpha}$  (Mabude et al. 2021). In Lu (2017), the  
 428 GWMA statistic  $Y_i$  is the input of the CUSUM chart, i.e.

$$Y_i = \sum_{t=1}^i \left( q^{(t-1)\tilde{\alpha}} - q^{t\tilde{\alpha}} \right) x_{i-t+1} + q^{i\tilde{\alpha}} \cdot Y_0, \quad (8a)$$

429 and

$$C_i^+ = \max(0, Y_i - (\mu_Y + K) + C_{i-1}^+), \quad (8b)$$

430 where  $Y_0 = \mu_Y$  and  $C_0^+ = 0$ .

431

432 First, we define constant slack value  $K = k \cdot \sigma_Y$  and threshold  $H = h \cdot \sigma_Y$ . The hyperparameter setting  
 433  $\tilde{\alpha} = 0.9$ ,  $q = 0.2$ ,  $k = 1$ , and  $h = 41$  led to detection of all leaks, but FPs for leak 3 and 9.

434 In general, the slack and threshold values can be time-dependent based on iterative approximations  
 435 of mean and standard deviation of the GWMA statistic  $Y_i$ . We present the results for an alternative  
 436 setting of the slack and threshold values: The standard deviation  $\sigma_y$  of the in-control set is substantially  
 437 higher for some of the processes, including those of leaks 3 and 9, for which a false alarm is raised using  
 438  $H = h \cdot \sigma_Y$ . Therefore, an alternative approach to set the threshold was chosen to amplify the increase of  
 439  $H$  with increased  $\sigma_y$ , where  $H = c_1 \cdot \sigma_y^{c_2}$ , and constants  $c_1 = 1443.8$  and  $c_2 = 1.65$ . The results are listed  
 440 in Figure 3 (method *gw*).

441 While the GWMA-CUSUM methods allows for a flexible weighting, the hyperparameter setting requires  
 442 a more intensive tuning. Leaks 3 and 9 could only be correctly detected by the alternative threshold  
 443 setting, and tuning the constant parameters again requires phase II data. However, more elegant ways to  
 444 adaptively set the threshold, called adaptive methods, could be a promising way to approach this problem.  
 445 Additionally, leak 9 should be rather insensitive to outliers, whereas the tuning of the GWMA-CUSUM  
 446 method is done to be more sensitive towards small shifts. This is not a problem of normality, but it occurs  
 447 as very differently sized leakages should be detected, while remaining robust towards outliers. Similar to  
 448 method *w*, method *gw* is not designed for non-normal data with outliers, and this limits the identification  
 449 of a global hyperparameter setting which allows for an increased sensitivity towards small shifts. For  
 450 example, increasing  $q$  for a fixed  $\tilde{\alpha}$  leads to more sensitive statistics, but increases the FP rate across all  
 451 leaks.

452 Nonparametric & adaptive CUSUM (adn)

453 Based on the results of method *gw*, nonparametric and adaptive methods are investigated in the following.  
 454 Liu et al. (2014) propose a nonparametric & adaptive CUSUM control chart in case both the underlying  
 455 distribution and the magnitude of shifts is unknown. The chart combines an adaptive approach that  
 456 estimates the current mean shift  $\hat{\delta}_i$  by a modification of the EWMA statistic and the use of standardized  
 457 sequential ranks  $R_i^*$  to circumvent assumptions about the underlying distribution.

458 Define  $R_i^* = \frac{\sum_{t=1}^i \mathbb{I}\{x_t \geq x_{t-1}\} - (i+1)/2}{((i+1)(i-1))/12}$ , then the upper-side CUSUM statistic is given as

$$C_i^+ = \max(0, (R_i^* - K_i)/\tilde{h}(K_i) + C_{i-1}^+), \quad (9)$$

459 where the slack value  $K_i = \frac{1}{2} \hat{\delta}_i$ , and  $\tilde{h}(K_i)$  is an operating function based on a predefined  $ARL_0$ .

460 The iterative approximation of the current mean shift and use of sequential ranks allow for a self-starting  
 461 scheme, i.e., no in-control data is needed. Theoretically, threshold  $H$  and the operating function  $\tilde{h}$ , based  
 462 on  $ARL_0$ , can be estimated using an arbitrary synthetic in-control distribution, as non-parametric schemes  
 463 should exhibit the same  $ARL_0$  properties for any underlying distribution. The current mean shift requires  
 464 a first estimate of the mean shift,  $\hat{\delta}_0^+$ , which potentially influences the detection performance.

465 If no knowledge of shift magnitude is available,  $Y_i = \frac{R_i^* + R_{i-1}^*}{2}$ ,  $\hat{\delta}_i = \max(\hat{\delta}_0, Y_i)$  and  $\hat{\delta}_0 = 0.7$  are  
 466 recommended. Here we adopt this setting, and assess the leak detection performance for different  $ARL_0$ .  
 467 The results are shown in Figure 5. No false alarm is raised using this method. Six leakages are not detected  
 468 for  $ARL_0 = 100, 200$ , and choosing  $ARL_0 = 30, 50$  still results in two undetected leaks. Lowering the  
 469 threshold  $H$  to an empirical value leads to detection of all leaks without raising FPs. All TTD results are  
 470 shown in Figure 3 (method *adn*). While two leaks (3 and 8) are not detected with an  $ARL_0 = 30$  and  
 471 the respective  $H$ -value, and are only detected when choosing a low empirical value, the  $C^+$  statistic is  
 472 very reliable for the chosen method, as no false alarms are raised without hyperparameter tuning based  
 473 on (potentially unavailable) in-control data. An alarm is raised only after a significant increase of the  
 474  $C^+$  statistic after the change point. However, an  $ARL_0 = 30$  is lower than typical values. This indicates  
 475 that the theoretical relation between  $ARL_0$  and FP rate does not hold for the monitored processes.  
 476 As the proposed CUSUM method assumes independent samples, a possible explanation is the effect of  
 477 autocorrelation on the true run length. Moreover, outliers and fluctuations of the distribution due to  
 478 operational variability are common for leakage detection problems.

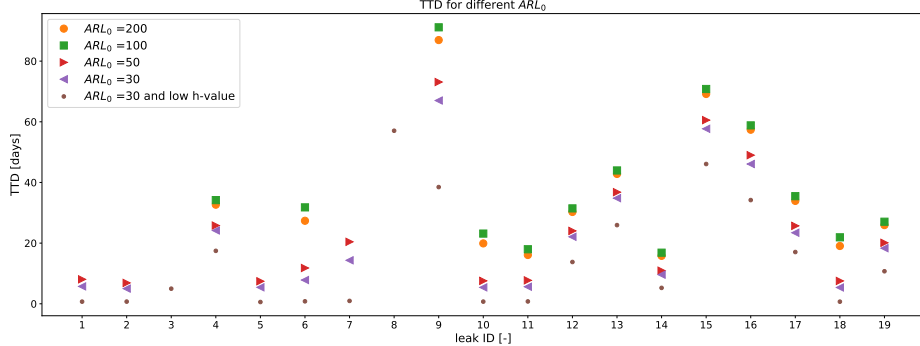


*Figure 5: TTD for different in-control average run lengths  $ARL_0$ : the represented TTD is obtained using nonparametric and adaptive CUSUM (method adn) for thresholds based on  $ARL_0 = 200, 100, 50, 30$  and additionally for a heuristic  $h$ -value, for all respective 19 leaks.*

#### 479 Nonparametric & adaptive CUSUM for arbitrary change (ac)

480 Nonparametric and adaptive methods seem promising as they can detect changes of different magnitude,  
 481 do not rely on a normality assumption, and do not need calibration data samples. While GWMA-CUSUM  
 482 searches for changes in the mean, other charts also track scale changes of the distribution, which could  
 483 be interesting for incipient leaks. Hence, we here test a nonparametric & adaptive method for arbitrary  
 484 changes (Li 2021) (method ac): the method detects increases and decreases in both location and scale  
 485 parameters. The method includes a built-in post-signal diagnostic function to identify the type of change  
 486 after an alarm was raised. Instead of assuming underlying in-control and out-of-control distributions, the  
 487 method employs data categorization based on quantiles of a reference distribution. While the in-control  
 488 quantiles are sequentially updated, we consider an initial sample of  $m_{IC} = 200$  data points (less than a  
 489 day) to get an initial estimate of the quantiles. The quantiles are used to derive  $d$  left-to-right regions  
 490 for the location change and center-to-outward regions for scale changes, respectively. Based on the  
 491 regions, a multinomial RV which indicates the categorization information of the current observation. In  
 492 order to include the ordering information (in time) of the observations, a dependent Bernoulli RV ( $Z$ ) is  
 493 computed based on cumulative sums of the multinomial RV which indicates the categorization information.  
 494 The proposed CUSUM statistic employs the log-likelihood ratio based on  $Z$ , i.e., the logarithm of the  
 495 out-of-control over in-control probability of  $Z$ . Here, the out-of-control probabilities are derived with a  
 496 Bayesian estimator, where the prior probability of the out-control-distribution is given by parameters of  
 497 the Dirchilet distribution (Li 2021). Those can either be obtained by simulation, if prior knowledge of the  
 498 change point is available, or by simulations using normal distribution.

499 The regions used for data categorization differentiate the CUSUM statistic for location or scale changes.

Additionally, the upper-side and lower-side statistics use different prior probabilities for the Dirchilet distribution. Hence, a total of four statistics are simultaneously computed, i.e.,  $C_i^{1+}$  for positive location changes,  $C_i^{1-}$  for negative location changes,  $C_i^{2+}$  for positive scale changes, and  $C_i^{2-}$  for negative scale changes. The threshold is set based on  $ARL_0$ . However, for  $d = 10$  and in-control reference data  $m_{IC} = 200$ , FPs were rasied for almost all leaks using the theoretical threshold for  $ARL_0 = 100$ . Hence, an empirical threshold  $H = 5000$  was set. An alarm is raised only if the  $C_1^+$  statistic exceeds threshold  $H$ . The results are listed in [Figure 3 \(method ac\)](#). While the scale changes statistics  $C_2^+$  and  $C_2^-$  do not showcase a reliable performance across all leaks, they lead to an earlier detection of some incipient leaks, e.g., leak 8, as can be seen Figure 6.

While monitoring of scale changes seems to be valuable for some leaks, setting of the threshold based on the run length was again not possible for this method. Similar to method *adn*, possible explanations are the presence of autocorrelation, outliers, and fluctuations due to operational variability. Additionally, the prior distribution used to estimate the out-of-control probabilities does effect the performance of the proposed control chart. In particular, it favors the detection of either small or large changes ([Li 2021](#)).

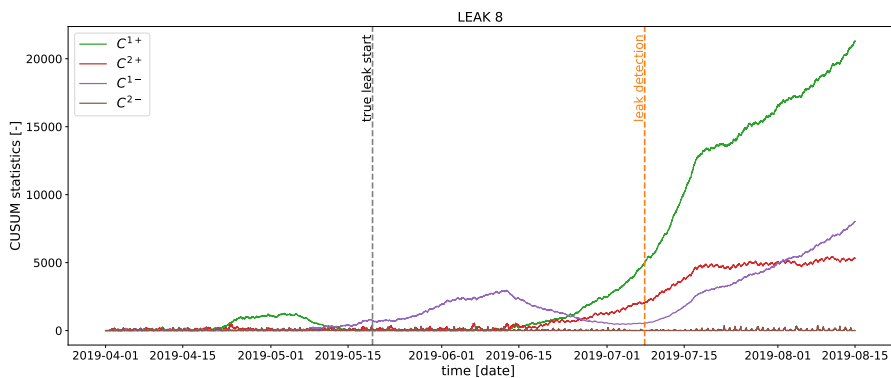


Figure 6: CUSUM Statistics  $C_1^+$ ,  $C_2^+$ ,  $C_1^-$ , and  $C_2^-$  obtained for method *ac* for leak 8 are shown. The leak is detected on 2019-07-07 when using  $C_1^+$  (vertical orange dotted line), however, the TTD could be much shorter when employing scale statistics.

#### Nonparametric & adaptive CUSUM for autocorrelated data (corr)

If assumptions of control charts are not met, their performance might be unreliable. In particular, autocorrelation might influence the average run length ([George and Box 2000](#)). While applying control charts to residuals of fitted models might mitigate autocorrelation, insufficient models, or fluctuations due to unmodeled operational variability can still lead to autocorrelated MRE time series. Indeed, some of

519 the investigated MRE data can be identified as autocorrelated according to the Durbin-Watson statistic  
 520 of the in-control data (see Section A.3 for details). In Li and Qiu (2020), a general CUSUM scheme  
 521 is suggested for autocorrelated data. In a first step, the data is de-correlated based on the Cholesky  
 522 decomposition (Higham 2009, cf.) under the assumption of stationary covariance. Using a small-to-  
 523 moderate in-control data set consisting of  $m_{IC}$  samples, an initial estimate of mean and covariances. Two  
 524 observations are assumed to exhibit no covariance if they are more than a maximum number of steps  
 525 apart, which is given by  $b_{max} \in \mathbb{N}^{\geq 1}$ . Based on the estimates of mean and covariance, the data is then  
 526 recursively decorrelated. During phase II monitoring, the estimates are recursively updated, and the  
 527 current observation is decorrelated with all  $T_{i-1}$  previous observations. This number is given by the spring  
 528 length  $T_i$ , i.e. the number of observations between the current time and the last time point at which the  
 529  $C^+$  was zero. In short, the Cholesky decomposition recursively produces uncorrelated and standardized  
 530 samples  $x_1^*, x_2^*, \dots$ . These samples are then paired with a nonparametric and adaptive method, of which we  
 531 discussed two approaches, i.e., methods *adn* and *ac* in this work. The latter uses data categorization and  
 532 an Bayesian estimate of the out-of-control probability which depends on the chosen prior. In comparison,  
 533 method *adn* requires less assumptions. In the following, the recursive Cholesky decomposition step (Li  
 534 and Qiu 2020) is combined with the nonparametric and adaptive method *adn* (Liu et al. 2014).

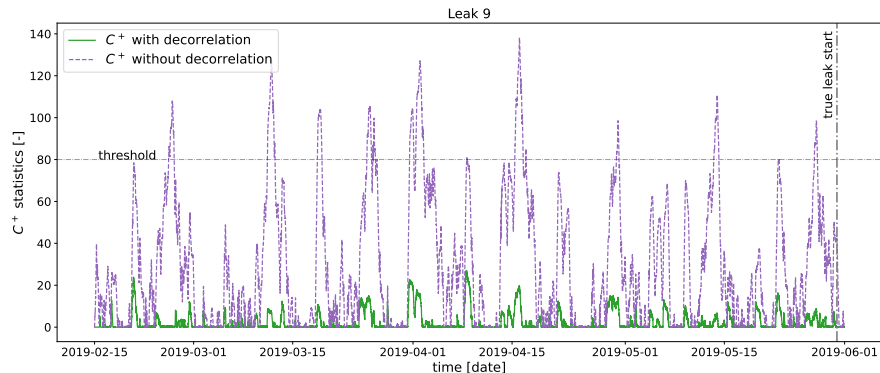


Figure 7: CUSUM Statistic for leak 9: the respective  $C^+$  statistics with (green) and without (purple) decorrelation step is visualized until the true leak 9 starts. The decorrelation step reduces the sensitivity of the statistic due to random fluctuations.

535 The decorrelation does not result in an improved detection for theoretical threshold values based on the  
 536  $ARL_0$ , possibly as removing the autocorrelation cannot account for all random variations and outliers in  
 537 the data set. Nonetheless, the decorrelation step decreases fluctuations of the  $C^+$  statistic before the change  
 538 points. This can be seen in Figure 7, where the respective  $C^+$  statistics with and without decorrelation

step are plotted until the true leak starts. As random fluctuations of the  $C^+$  statistic are significantly smaller when a Cholesky decorrelation is performed, a lower empirical threshold  $H$  can be chosen, which in turn reduces the TTD. Nevertheless, the  $C^+$ -statistic increases less due to the decorrelation step. This is desireable, if the time series exhibits high fluctuations but not otherwise. The  $C^+$  statistics for all leaks, for which decorrelation was performed, are shown in Figure 8. For all leaks, the  $C^+$ -statistic remain flat before the true leak start due to the decorrelation. After the change point, the statitics still rapidly increase. Nevertheless, this increased might be delayed due to decorrelation, which can be seen for leak 9.

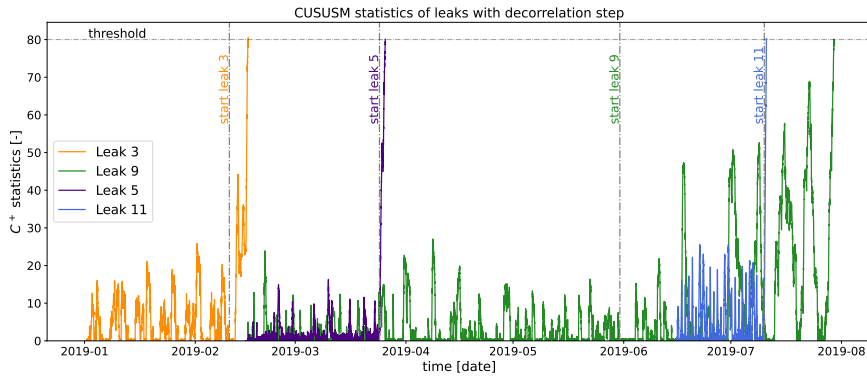


Figure 8: CUSUM statistic of leaks with decorrelation step: the  $C^+$  statistics obtained with method *corr* are represented for all leaks. An alarm is raised, if the respective statistic exceeds the threshold  $H = 80$ .

The numerical results for this method are shown in Figure 3 (method *corr*), where a constant threshold  $H = 80$  was used across all leaks, and a Cholesky decomposition with  $b_{max} = 10$  and  $m_{IC} = 200$  was paired with method *adn* for all leaks that exhibit autocorrelation based on the Durbin-Watson statistic. For method *adn*, the same hyperparameters as before are chosen, i.e.,  $\hat{\delta}_0 = 0.7$  as an initial guess of the mean shift and  $ARL_0 = 30$  for the operation function.

## 5 Discussion and comparative analysis

The seven methods (*t*, *tr*, *w*, *gw*, *adn*, *ac*, *corr*) we selected for comparative analysis represent potential techniques able to address the identified challenges related to SPC for leakage detection, namely unknown & non-normal underlying distributions, robustness towards outliers & random fluctuations, unknown mean change & detection sensitivity towards small or non-constant changes, and autocorrelated data. Here, we evantually compare them based on their leak detection performance, as well as data and training requirements.

558 First, two techniques are tested to deal with non-normal data, i.e., transformations (method  $t$ ) and  
559 their combination with robust statistics (method  $tr$ ). While the Box-Cox transformation is one of the  
560 few techniques applied to leakage detection (Buchberger and Nadimpalli 2004), results show it does  
561 not necessarily mitigate the effect of outliers. In combination with robust statistics, slight detection  
562 improvement was made by avoiding a FP for leak 3, however, still no reliable overall detection is achieved  
563 across all leaks. Additionally, an in-control data set is needed for selecting an appropriate Box-Cox  
564 parameter for the transformation. In practice, no or only a small (and possibly unrepresentative) in-control  
565 set might be available. The hyperparameter setting of the slack value and threshold remains challenging,  
566 as high variation of the run length can be observed for each leak, along with variable average run length  
567 across all processes.

568 To increase sensitivity towards small (incipient) leaks, we tested a weighted technique (method  $w$ )  
569 and a combination of CUSUM with GWMA (method  $gw$ ). However, both methods introduce additional  
570 hyperparameters and the subsequent tuning again requires in-control data. Our comparative analysis  
571 suggests that these hyperparameters must be tuned individually for each time series to leverage the methods  
572 capability for increased detection performance. This in turn may hinder their practical applicability for  
573 leakage detection. In order to find a global hyperparameter setting, the threshold setting for method  $gw$   
574 was adjusted **ad hoc**. This led to detection of all leaks, however, transferability to other test cases cannot  
575 be guaranteed.

576 The results of the **ad hoc** threshold adjustment motivates the use of adaptive techniques, which  
577 **embed** iterative threshold adaptations instead of fixed control limits. A naive approach is the use of  
578 multiple CUSUM statistics, which has previously been used for leakage detection (Bakker, Jung, et al.  
579 2014). However, each statistic still requires a fixed control limit, which corresponds to an assumption of a  
580 specified **constant** mean shift magnitude  $\delta$ . If **this constant cannot be properly set due to missing prior**  
581 **information about the mean shift size**, more advanced options make use of recursive estimation of the  
582 mean shift or out-of-control distribution based on iteratively available phase II process data. At the same  
583 time, nonparametric methods avoid the normality assumptions, either by use of sequential ranks or data  
584 categorization. Method  $adn$  combines sequential ranks and expected mean shift estimation, while method  
585  $ac$  employs data categorization and out-of control-probabilities.

586 For both methods  $adn$  and  $ac$ , respective global hyperparameter settings could be found that lead to  
587 detection of all leaks with average TTD (aTTD) of 14.6 and 14 days. However, both indirectly incorporate

588 information about a belief of mean shift size, which might impact their practical use cases: in case of *adn*,  
589 the adaptive threshold setting requires setting an *estimated* initial mean shift  $\hat{\delta}_0$ . Smaller values for  $\hat{\delta}_0$   
590 increase detection capabilities of small leaks and vice versa. In case of scant knowledge, the recommended  
591 setting  $\hat{\delta}_0 = 0.7$  performed well for all leak sizes. In contrast, method *ac* utilizes a Bayesian estimate of  
592 the out-of-control probability. Even though the recommended prior in case of scant knowledge produced  
593 good results for method *ac*, Bayesian estimates are typically heavily influenced by the chosen prior. An  
594 assessment of the overall effect of the prior across all time series is not straightforward. Even though  
595 Bayesian CUSUM methods (Javed et al. 2024; Heard and Turcotte 2017; Ali 2020; Bourazas et al. 2023)  
596 are not part of this comparison, initial tests of a Bayesian CUSUM method, employing a prior distribution  
597 based on in-control data, have shown that the required size of the in-control set needed to form a suitable  
598 prior differs substantially for the different leaks of the test case. Nonetheless, assuming availability of a  
599 large in-control set, Bayesian CUSUM methods potentially provide an elegant framework to incorporate  
600 information of the specific in-control distribution into the CUSUM control chart.

601 While both *adn* and *ac* adopt a self-starting scheme,  $m_{IC} = 200$  initial data points are used as a small  
602 in-control group for *ac* to derive an initial estimate of the in-control quantiles. Unlike the other methods,  
603 arbitrary change can be detected with method *ac*, referring to change in the location as well as the scale  
604 parameter of the distribution. Some results indicate that tracking the scale parameter increases detection  
605 performance for small incipient leaks, such as leak 8.

606 In general, *nonparametric* methods such as *adn* and *ac* require less hyperparameter tuning. However, the  
607 theoretical thresholds are still based on the average in-control run length. For example, the theoretical  
608 threshold for method *adn* is derived based on a desired  $ARL_0$  using an arbitrary in-control distribution.  
609 Using  $ARL_0$  might lead to practical problems for the leakage detection problem (see, for more detail,  
610 Appendix A.2). Indeed, the theoretical threshold for method *adn* led to no detection of some leaks within  
611 the simulated time period, while no false alarms were raised. Since false alarms are avoided using the  
612 theoretical threshold, one practical solution is using it initially and update it based on emerging historical  
613 phase II data, as previously suggested for leakage detection (Eliades and Polycarpou 2012). Indeed, for  
614 both methods *adn* and *ac*, global empirical thresholds could be chosen based on the leakage time series  
615 data, such that all leakages are detected without raising false alarms.

616

617 Nonparametric & adaptive techniques effectively address simultaneously the problem of variable leak

618 sizes, no or little in-control data, and non-normal distributions. However, methods *adn* and *ac* still assume  
619 independence of data points. LILA employs the CUSUM to MRE time series, which is a common method  
620 to mitigate autocorrelation. Yet, this approach can have limited reliability in leakage detection and high  
621 model errors when unknown water demands occur in some WDN nodes. For the reasons mentioned  
622 above, the implementation of method *adn* is easier for the leakage detection problem. Therefore, it was  
623 combined with a decorrelation approach based on the Cholesky-decomposition for all MRE that exhibit  
624 autocorrelation, presented as method *corr*. To test the presence of autocorrelation and get an initial  
625 estimate of the moments needed for the decorrelation, a small in-control group of  $m_{IC} = 200$  samples  
626 needs to be employed. In spite of that, the additional decorrelation step resulted in decreased  $C^+$  statistics  
627 before the change point. This effect is particularly interesting because it affects those time series whose  
628 CUSUM statistic of other methods was subject to large random fluctuations, so that either a false alarm  
629 was raised or higher global control limits had to be selected. One example is Leak 9, where results suggest  
630 that the decorrelation step increases the reliability of the  $C^+$  statistic, even though it cannot remove  
631 all random fluctuations and outliers. As the decorrelation step can be assumed to decrease the initial  
632 effect of incipient leaks, the use of the Durbin-Watson statistic to test for autocorrelation is a useful  
633 easy-to-implement statistical test to decide whether the decorrelation step is necessary.

634 We ultimately complete the above analysis based on TTD with a compilation of various performance  
635 metrics for the selected CUSUM-based SPC methods. The results for each method are reported in Table  
636 4, where recall, precision, and the  $F_1$ -score, which are standard classification metrics (Lever 2016), are  
637 calculated. [The definition of the metrics is reported in Section A.1](#).

638 [Table 4 shows the aTTD and metric results for each method, where the best values are highlighted](#). The  
639 empirical hyperparameter setting limits a complete comparison based on these metrics. [For example](#),  
640 [while the ad hoc threshold setting of \*gw\* leads to a detection of all leaks, its transferability to online](#)  
641 [leakage detection without knowledge of the phase II data is limited. Still, the lower recall, precision, and](#)  
642 [F<sub>1</sub>-scores for the standard method, \*t\*, \*tr\*, and \*w\* indicate a lower reliability of these methods, compared to](#)  
643 [more advanced GWMA and nonparametric and adaptive methods. In contrast, methods \*adn\*, \*ac\*, \*corr\*](#)  
644 [result in more reliable performance. The mitigation of random fluctuations of the  \$C^+\$  statistics through](#)  
645 [decorrelation increases the reliability of method \*corr\*. The decorrelation step results in an aTTD of 14.4](#)  
646 [days. In fact, decorrelation can lead to a delayed increase of the  \$C^+\$  statistic. Therefore, it should only be](#)  
647 [used if high random fluctuations are expected – in practice, this is the case if, e.g., irregular demands are](#)

present. For the L-town case study irregular demands occur in DMA C, and concerns leak 3 and 9 of the 2019 benchmark set. Indeed, the decorrelation step resulted in improved  $C^+$  statistics for the two leakages, as has been shown in Figures 7 and 8. All in all, the use of methods *adn* and *corr* with an initial theoretical threshold that is updated based on historical data, promises the greatest reliability for all identified problems of leakage detection.

The selected CUSUM-based methods of this comparison are tested on the MRE time series of the published LILA code, which, as mentioned in Section 2, relied on manually-selected training times and sensor combinations for each leak in the published code (Daniel, Pesantez, et al. 2022). We have conducted further tests, where the linear regression was carried out using different systematic training times and a variety of sensor combinations. Preliminary results not reported here suggest that *adn*, *ac*, and *corr* are performing robust towards these changes. This further underlines their usability for (semi-supervised) leakage detection methods in real-case scenarios, where training times cannot be chosen manually, and the best sensor combination for detecting a specific leak is unknown a priori.

*Table 4: Performance metrics for the selected CUSUM-based SPC methods for comparative analysis.*

Method acronym	Method	aTTD [days]	recall [-]	precision [-]	$F_1$ [-]
	standard CUSUM	<b>9.1</b>	<b>1</b>	0.89	0.94
<i>t</i>	transformed CUSUM (Figueiredo and Gomes 2003)	12.5	0.94	0.89	0.91
<i>tr</i>	transformed & robust CUSUM (Figueiredo and Gomes 2003; Nazir et al. 2013)	11.6	<b>1</b>	0.95	0.97
<i>w</i>	weighted CUSUM (Shu et al. 2008)	13.8	0.94	0.89	0.91
<i>gw</i>	GWMA-CUSUM (Lu 2017)	12.8	<b>1</b>	<b>1</b>	<b>1</b>
<i>adn</i>	nonparametric & adaptive CUSUM (Liu et al. 2014)	14.6	<b>1</b>	<b>1</b>	<b>1</b>
<i>ac</i>	nonparametric & adaptive CUSUM for arbitrary change (Li 2021)	14.0	<b>1</b>	<b>1</b>	<b>1</b>
<i>corr</i>	nonparametric & adaptive CUSUM for autocorrelated data (Liu et al. 2014; Li and Qiu 2020)	14.4	<b>1</b>	<b>1</b>	<b>1</b>

## 6 Conclusion and recommendations for SPC in leak detection

This work is concerned with the problem of promptly and reliably detecting leakages in water distribution networks based on sensor data. While model-based detection methods are generally accurate, they require a calibrated hydraulic model of the water distribution network, which is not often available. Several data-driven methods have thus been proposed in the literature to abstain from sophisticated hydraulic modeling, many of them relying on statistical process control techniques to detect change points on sensor

667 data time series, which signify the occurrence of a leak. However, several practical challenges emerge from  
668 existing integration of SPC methods in leakage detection, including non-normal distributions, outliers,  
669 random fluctuations, and autocorrelated data. Additionally, different change/leak magnitudes and little  
670 in-control data for calibration are common for leakage detection. To address these challenges, here we  
671 contribute a systematic and comparative analysis of advanced SPC techniques based on cumulative sum  
672 (CUSUM) charts for leakage identification in water distribution networks. Starting from an extensive  
673 literature review of approximately 100 SPC publications, we select advanced state-of-the-art CUSUM-based  
674 methods, integrate them as the SPC step for leak identification into a state-of-the-art the data-driven leak  
675 identification method “LILA” (Daniel, Pesantez, et al. 2022), and test their detection performance on the  
676 L-Town benchmark WDN released as part of the BattLeDIM (Vrachimis et al. 2022). Based on the results  
677 of our comparative analysis, we ultimately formulate recommendations on potential, requirements, and  
678 limitations for practical usage of the respective methods in the context of leak detection under different  
679 use cases. These recommendations are summarized in Table 5.

680 Three main outcomes emerge from our analysis. First, increasing detection performance towards small  
681 incipient leaks has been highlighted as an important topic for future research (Wan et al. 2022; Wu et al.  
682 2024). In this work, the use of a weighted CUSUM and GWMA-CUSUM method highlights their potential  
683 for improved leak detection. However, the FP rate might increase due to sensitivity of the methods  
684 towards random changes. Furthermore, both methods introduce additional hyperparameters in comparison  
685 with standard or transformation-based CUSUM, thus hampering ease of training and transferability. A  
686 possible starting point for methods that combine techniques for robustness and weighting could be the  
687 distribution-free mixed GWMA-CUSUM chart (Mabude et al. 2021). Method *ac* in this work includes  
688 tracking of scale changes of the distribution, which also showed sensitivity towards incipient leaks.

689 Second, [Wan et al. \(2022\)](#) also raise the question how to handle spurious outliers. We show that  
690 the robust statistics used for method *tr* achieve superior results to the standard CUSUM method, but  
691 are not sufficient for all random variations. Furthermore, these methods require an in-control dataset  
692 to set the transformation parameters and hyperparameter setting remains challenging. In contrast, the  
693 nonparametric and adaptive methods (*adn* and *ac*) show improved performance as they account for  
694 different change magnitudes, and adapt to non-normal distributions, guaranteeing better transferability.

695 If all of the identified SPC problems for leakage detection occur, the most robust results are achieved  
696 with nonparatic and adaptive CUSUM for autocorrelated data (method *corr*). It combines nonparametric,

697 adaptive CUSUM control charts with optional decorrelation. Though not all random variations can be  
 698 expected to be removed, this lead to decreased fluctuations of the  $C^+$  statistic before the true change  
 699 point. This results in substantially increased reliability and transferability to new detection problems.

700 While control charts might require specifying multiple hyperparameters, method *corr* only requires  
 701 setting the control-limit. Starting from a theoretical threshold based on the average in-control run length,  
 702 a practical solution involves its adaption based on (emerging) historical data. Further investigations may  
 703 include techniques used for multivariate data (Woodall and Ncube 1985), and dynamic probability control  
 704 limits (Steiner et al. 2000; Zhang and Woodall 2015). The latter are developed to mitigate the effect of  
 705 variable  $ARL_0$  due to rare events. Multivariate data, on the other hand, though not investigated in this  
 706 work, is commonly monitored by multiple univariate control schemes. If a global threshold is applied, the  
 707 problem becomes similar to a global threshold for the respective MRE time series in this work.

708 This work eventually advances water loss management by addressing both theoretical and practical  
 709 aspects. Theoretically, it fills a gap in the literature as, to our knowledge, no comparative analysis of  
 710 change point detection methods for leak detection has been conducted. Practically, our findings offer  
 711 actionable recommendations, guiding the selection of appropriate change point detection methods based  
 712 on real-world considerations such as data characteristics, performance expectations, and specific boundary  
 713 conditions.

*Table 5: Use-cases, requirements, and limitations of selected CUSUM-based SCP methods for practical usage in leak detection in WDNs.*

Method acronym	Use-cases	Requirements	Limitations
<i>t</i>	approximate normality for non-normal distributions	in need of sufficiently large in-control set, hyperparameter tuning for each time series needed	not robust towards outliers, fixed shift size to be detected, not for autocorrelated data
<i>tr</i>	approximate normality, & mitigate influence of outliers	in need of sufficiently large in-control set, hyperparameter tuning for each time series needed	fixed shift size to be detected, not for autocorrelated data
<i>w</i>	detection within restricted time window: increased sensitivity towards small shifts	in need of sufficiently large in-control set, hyperparameter tuning for each time series needed	not robust towards outliers or non-normality, fixed shift size to be detected, not for non-normal & autocorrelated data
<i>gw</i>	increased sensitivity towards small leaks, flexible weighting of data points	in need of sufficiently large in-control set, hyperparameter tuning for each time series needed	not robust towards outliers or non-normality, fixed shift size to be detected, not for non-normal & autocorrelated data
<i>adn</i>	detection of range of shift changes of unknown distribution	with no or little IC-data	not for autocorrelated data, for multiple processes empirical threshold might perform better
<i>ac</i>	detection of range of shift & scale changes of unknown distribution	with no or little IC-data	not for autocorrelated data, for multiple processes empirical threshold might perform better, in-control information might improve Bayesian estimate
<i>corr</i>	detection of range of shifts of unknown distribution for autocorrelated data	with little IC-data	for multiple processes empirical threshold might perform better, decorrelation step increases TTD of transient leaks: should only be used if needed

714 **A Appendix**

715 **A.1 Metrics**

716 In the following, the three performance metrics used in this work are formulated (Lever 2016).

717 Recall is given as the proportion of known positives that are predicted correctly. Precision measures the  
718 proportion of true positives (TP) to FP, and the  $F_1$ -score is the harmonic mean of Recall and Precision,  
719 where  $0 \leq F_1 \leq 1$ , and a larger  $F_1$ -score indicates better classification. These metrics are formulated as

$$\text{recall} = \frac{\text{TP}}{\text{TP} + \text{FN}}, \quad (10a)$$

$$\text{precision} = \frac{\text{TP}}{\text{TP} + \text{FP}}, \quad (10b)$$

721 and

$$F_1 = \frac{2 \cdot \text{recall} \cdot \text{precision}}{\text{recall} + \text{precision}}. \quad (10c)$$

722

723 **A.2 Note on in-control average run length  $ARL_0$**

724 The in-control average run length  $ARL_0$ , defined as the average number of iterations before a false alarm  
725 is given based on the in-control data. It is a common metric to compare different control charts, and  
726 can be used to choose an appropriate threshold parameter for a chosen slack value. A common choice is  
727  $ARL_0 = 370$  which corresponds to a FP risk  $r = \frac{1}{ARL_0} \approx 0.27\%$ .

728

729 Aside from analytical approximations, there are three main approaches to approximate the  $ARL_0$ , i.e.  
730 integral equation, Monte Carlo simulation and Markov Chain. Latter, initially proposed by Brook and  
731 Evans (Brook and Evans 1972), estimates  $ARL_0$  by discretization of the probability distribution of the  $C^+$   
732 statistic, where the transition probabilities are derived based on an in-control set. The integral equation  
733 method (Crowder 1987) derives  $ARL_0$  as a solution of an integral equation, which is solved numerically in  
734 most cases. Lastly, the Monte Carlo approach repeatedly generates sequences of charting statistics based  
735 on an in-control data set until the control limit is passed to determine the average of the recorded run  
736 lengths (Lim and Lee 2024).

737

For the leakage detection problem at hand, a universal hyperparameter setting across all MRE time series is desirable, as in-control data is not evaluated for each newly occurring leak. However, the values for the  $ARL_0$  associated to a specific hyperparameter setting varies between the processes, making a universal selection of hyperparameters for a constant  $ARL_0$  across all time series infeasable. This is shown in Figure 9, where, using the standard CUSUM method, the  $ARL_0$  is computed for  $k = 2$  and various values of the threshold parameter  $h$  for leak 1 and 3. We choose the Markov Chain method (Knoth 2021) and two Monte Carlo approaches (Lim and Lee 2024) to estimate the  $ARL_0$ . The first Monte Carlo method, labeled  $MCD$ , relies on Monte Carlo dropout. This approach drops the run length  $RL_i$  computed at simulation iteration  $i$ , if no alarm was raised within the generated sequence. However, this is only approximately true, if the drop out rate is not too high. The truncated Monte Carlo approach  $MCT$  instead records  $RL_i = m_{IC}$  in case no alarm is given, where  $m_{IC}$  is the length of the sequence. As no alarms are raised,  $ARL_0$  based on the truncated Monte Carlo approach approaches  $m_{IC}$ , and simultaneously, the  $MCD$  estimate becomes less reliable, as few simulation iterations lead to a recorded run length. In Figure 9, boxplots of the 5000 recorded run lengths, i.e. the set  $\{RL_i\}_{i=1}^{5000}$ , for  $k = 2$ ,  $m_{IC} = 865$ , and various  $h$ -values are shown. It can be seen, that the number of the raised alarms decreases significantly as larger values for  $h$  are chosen, and thus reducing the estimation accuracy. At the same time, the Markov Chain approach also leads to unreliable estimates of  $ARL_0$  in this case, as no transition probability for some states  $[0, H]$  of the  $C^+$  statistic can be estimated based on the in-control data.

756

If the threshold  $h$  would be chosen based on  $ARL_0 = 370$  for  $k = 2$ , the three methods ( $MCD$ ,  $MCT$ , and Markov Chain) still produce reliable results (see Figure 9). However, for the standard CUSUM methods, this leads to false alarms for all leakages. Thus, the FP risk is significantly higher than 0.27%. At the same time, the hyperparameter setting of  $k = 2$  and  $h = 4$  leads to estimation problems of the  $ARL_0$  as shown above. These robustness issues for practical issues, as well as negative effects the skewness of the run-length distribution are discussed in (Graham et al. 2014). Effects of estimation errors are investigated in (Jones and Steiner 2012). Additionally, there are multiple reasons why the required  $ARL_0$  exceeds the theoretical value, including autocorrelation, non-normality and outliers. Some of the investigated control charts mitigate the influence of these characteristics, as discussed in detail in Section 5. To still showcase the “best” possible performance of each method for this practical problem, an empirical hyperparameter setting based on TTD and FP was employed in this work. To realise this method in practice, historical

768 data would be needed to tune the hyperparameters. We discuss this as well in Section 5.

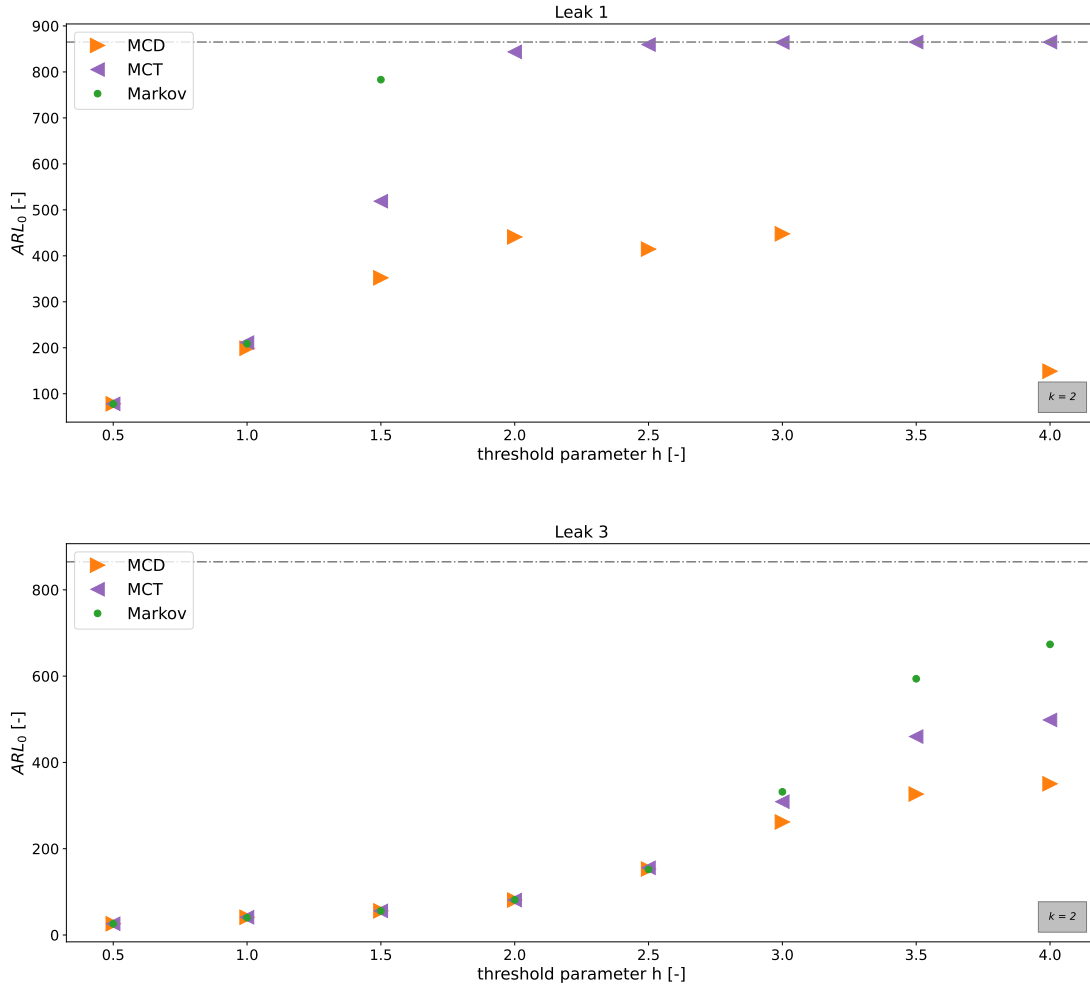


Figure 9: Estimation  $ARL_0$ : estimates of  $ARL_0$  using MCD, MCT, and Markov Chain are shown for leak 1 (upper Figure) and leak 3 (lower Figure) are shown. While similar estimation results of the three methods indicate reliable estimation, the respective  $ARL_0$  does not result in avoidance of false alarms: For example, leak 1 requires  $h \geq 2.5$  in order to not raise a FP, and leak 3 raises FP across all plotted hyperparameter settings and corresponding  $ARL_0$  estimates.

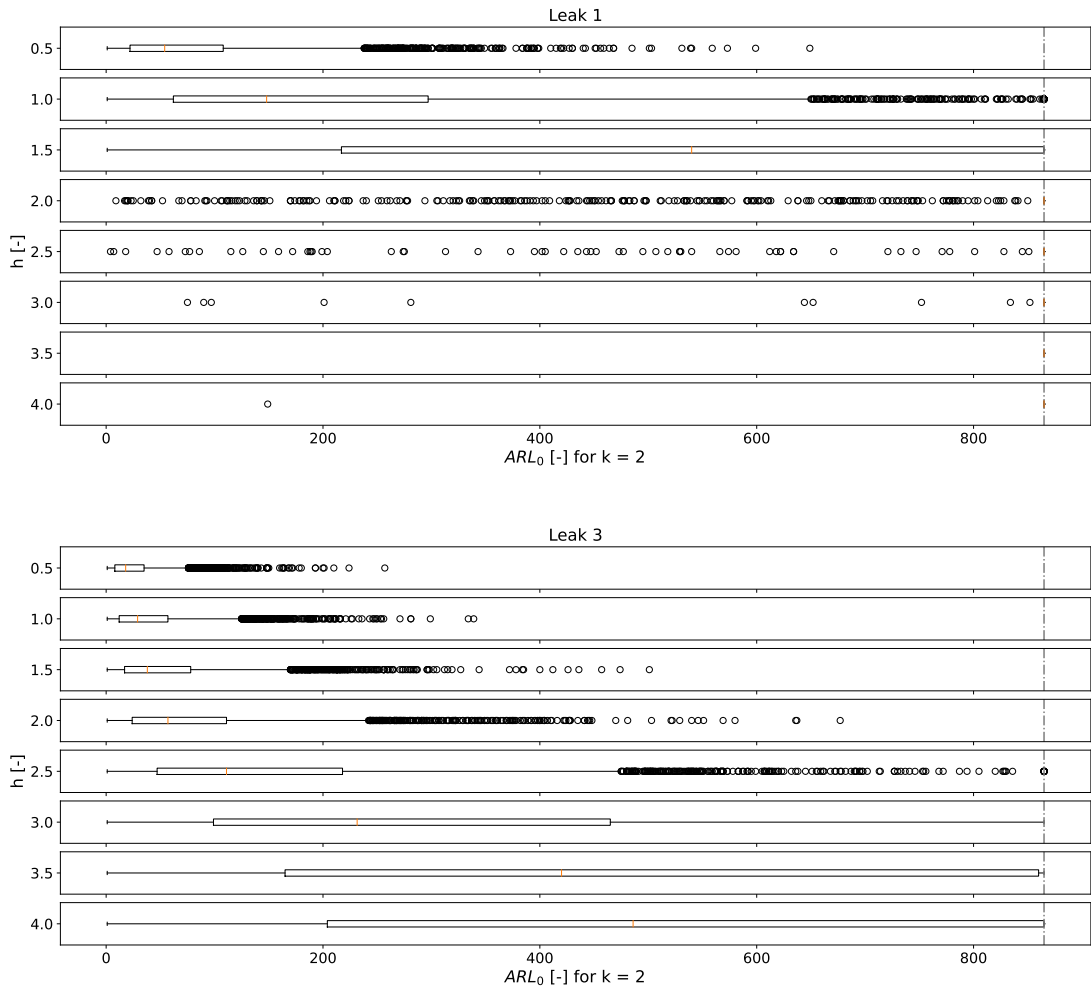


Figure 10: Boxplot of recorded run lengths, i.e. the set  $\{RL_i\}_{i=1}^{5000}$  for MC approaches: for different  $h$ -values and  $k = 2$ , this Figure shows the recorded run lengths for leak 1 (upper Figure) and leak 3 (lower Figure). As  $h$  increases, the number of usable recorded run-length decreases, which in turn increases the estimation error of MCD and MCT estimates.

769 **A.3 Statistical tests**

770 In order to test for the presence of autocorrelation, and non-normal in-control distributions, the Durbin-  
 771 Watson (Durbin and Watson 1992) and Kolmogorov-Smirnov (Massey 1951) tests are employed. For each  
 772 time series, the first three days (864 data points) are used as in-control data with exception of leak 16,  
 773 where the true leak starts on the second day, and thus only the first day (288 data points) is used.

774

775 Table 6 presents the results for the test-statistic  $t_{DW}$  of the Durbin-Watson test, and the p-value of  
 776 the Kolmogorov-Smirnov test. For former test, the time series is assumed to be uncorrelated if  $1.5 \leq t \leq 2$ .  
 777 Therefore, leaks 3,5,9, and 11 are assumed to exhibit autocorrelation. Similarly, for p-values  $p < 0.5$ , the  
 778 in-control distribution is assumed to be non-normal. Hence, leaks 1,3,6,9,13, and 18 are assumed to be  
 779 non-normal. Indeed, the histograms of the in-control data of leaks 3,9, and 18 are clearly non-normal,  
 780 while leaks 1,6, and 13 seem to be slightly non-normal (see Figure 11).

*Table 6: Statistical tests results*

Leak ID	type	Durbin-Watson test statistic $t_{DW}$	Kolmogorov-Smirnov p-value $p$
1	abrupt	2.07	<b>0.01</b>
2	abrupt	1.86	0.9
3	abrupt	<b>0.18</b>	<b>0.0</b>
4	incipient	1.98	0.36
5	abrupt	<b>1.31</b>	0.27
6	abrupt	2.03	<b>0.04</b>
7	abrupt	1.56	0.12
8	incipient	2.09	0.2
9	incipient	<b>0.16</b>	<b>0.0</b>
10	abrupt	1.98	0.38
11	abrupt	<b>0.91</b>	0.34
12	incipient	1.73	0.42
13	incipient	1.61	<b>0.04</b>
14	incipient	1.98	0.2
15	incipient	1.97	0.15
16	incipient	1.92	0.82
17	incipient	1.87	0.47
18	incipient	1.97	<b>0.0</b>
19	incipient	1.97	0.09

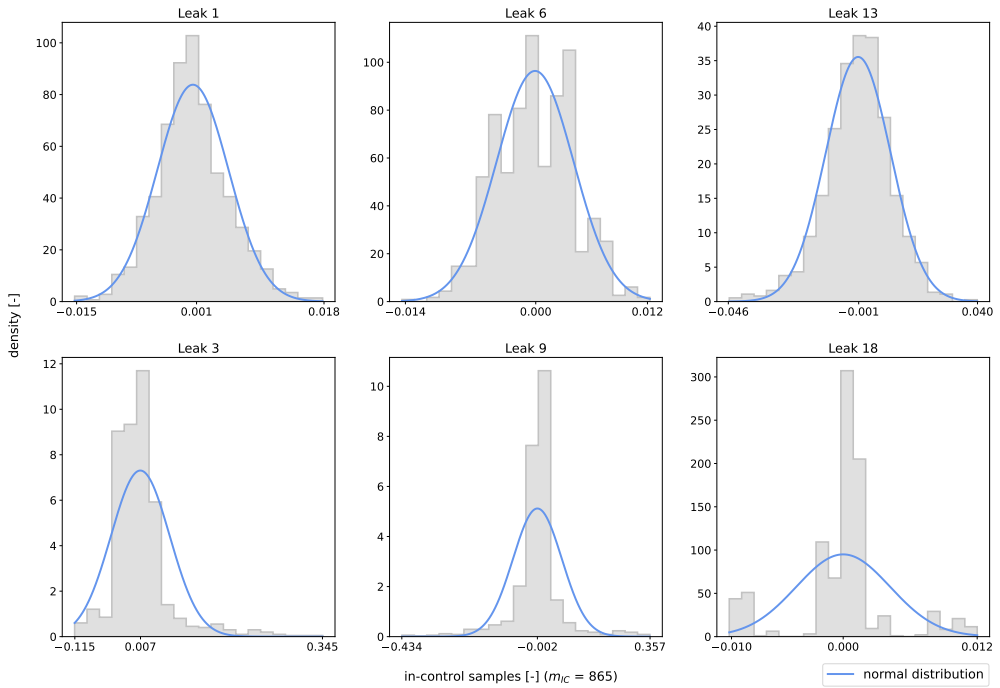


*Figure 11: Histograms of in-control distributions:* this Figure shows the histograms of the in-control distributions of leaks 1, 6, and 13 (upper Figure), and leaks 3, 9, and 18 (lower Figure). Compared to the normal distributions plotted, these distributions are non-normal based on the Kolmogorov-Smirnov test.

781 A.4 Nomenclature and Abbreviations

Table 7: Nomenclature

Symbol	Description
$b_{max}$	number of steps after which samples are assumed to be uncorrelated
$c$	Box-Cox constant
$c_1, c_2$	constants for alterantive threshold
$C^+$	positive CUSUM
$C_1^+, C_1^-, C_2^+, C_2^-$	positive CUSUM (shift), negative CUSUM (shift), positive CUSUM (scale), negative CUSUM (scale)
$d$	number of regions in which initial samples are divided
$F_1$	$F_1$ -score
$h$	threshold hyperparameter
$H$	threshold
$k$	slack value hyperparameter
$K$	slack value
$m_{IC}$	in-control data set size
$p$	p-value
$p$	precision
$q$	design hyperparameter
$Q_1, Q_2, Q_3$	-first, second, and third quartile
$r$	false positive risk
recall	recall
$R$	standarized sequential rank
$t_{DW}$	Durbin-Watson test statistic
$T$	spring length
$TM$	trimean
$w$	weighting factor
$W$	EWMA-estimator of mean
$x_1, x_2, \dots$	monitored samples with time index
$x_1^*, x_2^*, \dots$	uncorrelated and standardized samples with time index
$x_1^{BC}, x_2^{BC}, \dots$	Box-Cox transformed samples with time index
$Y_1, Y_2, \dots$	GWMA statistic with time index
$z_1, z_2, \dots$	z-score standardized and Box-Cox transformed samples with time index
$Z$	dependent Bernoulli random variable
$\alpha$	weight hyperparameter
$\bar{\alpha}$	adjustment hyperparameter
$\delta$	true constant mean shift
$\hat{\delta}$	approximation of mean shift
$\hat{\delta}_0$	initial approximation of mean shift (at time index 0)
$\mu_0, \sigma_0$	mean and standard deviation of in-control set of $x_1, x_2, \dots, x_{m_{IC}}$
$\mu_{tr}, \sigma_{tr}$	mean and standard deviation of Box-Cox transformed in-control set $x_1^{BC}, x_2^{BC}, \dots, x_{m_{IC}}^{BC}$
$\mu_Y, \sigma_Y$	mean and standard deviation of in-control set of GWMA statistic $Y_1, Y_2, \dots, Y_{m_{IC}}$
$\lambda$	Box-Cox variable

Table 8: Abbreviations

Abbreviation	Meaning
<i>ac</i>	method acronym: nonparametric & adaptive CUSUM for arbitrary change
<i>adn</i>	method acronym: nonparametric & adaptive CUSUM
aTTD	average time to detection
<i>ARL</i> <sub>0</sub>	in-control average run length
BattLeDIM	Battle of Leakage Detection and Isolation Methods
<i>corr</i>	method acronym: nonparametric & adaptive CUSUM for autocorrelated data
CUSUM	cumulative sum
DMA	district meter area
EWMA	exponentially weighted moving average
FN	false negative
FP	false positive
<i>gw</i>	method acronym: GWMA-CUSUM
GWMA	generally weighted moving average
IC	in-control
LILA	leakage identification and localization algorithm
MCD	drop-out Monte Carlo
MCT	truncated Monte Carlo
MRE	model reconstruction error
RL	run length
SCADA	Supervisory Control and Data Aquisition
SPC	stochastic process control
<i>t</i>	method acronym: transformed CUSUM
<i>tr</i>	method acronym: transformed & robust CUSUM
TP	true positive
TTD	time to detection
<i>w</i>	method acronym: weighted CUSUM
WDN	water distribution network

782 **A.5 Summary of hyperparameter selection**

*Table 9: Summary of hyperparameter selection.*

Method acronym	Method	Hyperparameters
	standard CUSUM	$h = 3, k = 2$
<i>t</i>	transformed CUSUM (Figueiredo and Gomes 2003)	$h = 3, k = 3$
<i>tr</i>	transformed & robust CUSUM (Figueiredo and Gomes 2003; Nazir et al. 2013)	$h = 3, k = 3$
<i>w</i>	weighted CUSUM (Shu et al. 2008)	$h = 3, k = 2, \alpha = 0.75$
<i>gw</i>	GWMA-CUSUM (Lu 2017)	$c_1 = 1443.8, c_2 = 1.65, \bar{\alpha} = 0.9, q = 0.2, k = 1, h = 41$
<i>adn</i>	nonparametric & adaptive CUSUM (Liu et al. 2014)	$\hat{\delta}_0 = 0.7, ARL_0 = 30,$ empirical threshold $H = 200$
<i>ac</i>	nonparametric & adaptive CUSUM for arbitrary change (Li 2021)	$m_{IC} = 200, d = 10,$ empirical threshold $H = 5000$
<i>corr</i>	nonparametric & adaptive CUSUM for autocorrelated data (Liu et al. 2014; Li and Qiu 2020)	$b_{\max} = 10, ARL_0 = 30, m_{IC} = 200, \hat{\delta}_0 = 0.7,$ empirical threshold $H = 80$

783 **Data Availability Statement**

784 Some or all data, models, or code generated or used during the study are available in online repositories in  
 785 accordance with funder data retention policies (Daniel et al. 2021; Vrachimis et al. 2022). Some or all  
 786 data, models, or code that support the findings of this study are available from the corresponding author  
 787 upon reasonable request.

788 **Acknowledgement**

789 This work is supported by the iOLE project, which receives funding from the Federal Ministry of Education  
 790 and Research (BMBF) within the funding measure “Digital GreenTech—Environmental Engineering meets  
 791 Digitalisation” as part of the “Research for Sustainability (FONA) Strategy” (funding code: 02WDG1689A).

792 **References**

- 793 Abbas, N., Riaz, M., and Does, R. (2013). “Mixed exponentially weighted moving average–cumulative sum charts for process monitoring”.  
 794 In: *Quality and Reliability Engineering International* 29.3, pp. 345–356.
- 795 Ahn, J. and Jung, D. (2019). “Hybrid statistical process control method for water distribution pipe burst detection”. In: *Journal of*  
 796 *Water Resources Planning and Management* 145.9, p. 06019008.
- 797 Ali, S. (2020). “A predictive Bayesian approach to EWMA and CUSUM charts for time-between-events monitoring”. In: *Journal of*  
 798 *Statistical Computation and Simulation* 90.16, pp. 3025–3050.

- 799 Ali, S., Pievatolo, A., and Göb, R. (2016). "An overview of control charts for high-quality processes". In: *Quality and reliability engineering international* 32.7, pp. 2171–2189.
- 800
- 801 Anjana, G. et al. (2015). "A particle filter based leak detection technique for water distribution systems". In: *Procedia Engineering* 119, pp. 28–34.
- 802
- 803 Bakker, M., Jung, D., et al. (2014). "Detecting pipe bursts using Heuristic and CUSUM methods". In: *Procedia Engineering* 70, pp. 85–92.
- 804 Bakker, M., Vreeburg, J., et al. (2014). "Heuristic burst detection method using flow and pressure measurements". In: *Journal of Hydroinformatics* 16.5, pp. 1194–1209.
- 805
- 806 Blesa, J. and Pérez, R. (2018). "Modelling uncertainty for leak localization in water networks". In: *IFAC-PapersOnLine* 51.24, pp. 730–735.
- 807 Boretti, A. and Rosa, L. (2019). "Reassessing the projections of the world water development report". In: *NPJ Clean Water* 2.1, p. 15.
- 808 Bourazas, K., Sobas, F., and Tsiamyrtzis, P. (2023). "Predictive ratio CUSUM (PRC): A Bayesian approach in online change point detection of short runs". In: *Journal of Quality Technology* 55.4, pp. 391–403.
- 809
- 810 Bozkurt, C., Firat, M., and Ateş, A. (2022). "Development of a new comprehensive framework for the evaluation of leak management components and practices". In: *AQUA—Water Infrastructure, Ecosystems and Society* 71.5, pp. 642–663.
- 811
- 812 Brook, D. and Evans, D. (1972). "An approach to the probability distribution of CUSUM run length". In: *Biometrika* 59.3, pp. 539–549.
- 813 Buchberger, S. and Nadimpalli, G. (2004). "Leak estimation in water distribution systems by statistical analysis of flow readings". In: *Journal of water resources planning and management* 130.4, pp. 321–329.
- 814
- 815 Chandola, V., Banerjee, A., and Kumar, V. (2009). "Anomaly detection: A survey". In: *ACM computing surveys (CSUR)* 41.3, pp. 1–58.
- 816 Crowder, S. (1987). "A simple method for studying run-length distributions of exponentially weighted moving average charts". In: *Technometrics* 29.4, pp. 401–407.
- 817
- 818 Daniel, I., Letzgus, S., and Cominola, A. (2021). *A high-resolution pressure-driven leakage identification and localization algorithm [Code]*. <https://github.com/SWN-group-at-TU-Berlin/LILA>, accessed on 10 April 2025.
- 819
- 820 Daniel, I., Pesantez, J., et al. (2022). "A sequential pressure-based algorithm for data-driven leakage identification and model-based localization in water distribution networks". In: *Journal of Water Resources Planning and Management* 148.6, p. 04022025.
- 821
- 822 Durbin, J. and Watson, G. (1992). "Testing for serial correlation in least squares regression. II". In: *Breakthroughs in Statistics: Methodology and Distribution*. Springer, pp. 260–266.
- 823
- 824 Eliades, D. and Polycarpou, M. (2012). "Leakage fault detection in district metered areas of water distribution systems". In: *Journal of Hydroinformatics* 14.4, pp. 992–1005.
- 825
- 826 Farah, E. and Shahrour, I. (2017). "Leakage detection using smart water system: Combination of water balance and automated minimum night flow". In: *Water Resources Management* 31, pp. 4821–4833.
- 827
- 828 Figueiredo, F. and Gomes, M. (2003). "Box-Cox transformations versus data modelling—robust charts in Statistical Process Control". In: *Notas e Comunicações CEAUL* 13, p. 2003.
- 829
- 830 — (2004). "The total median in statistical quality control". In: *Applied stochastic models in business and industry* 20.4, pp. 339–353.
- 831 Fox, S. et al. (2016). "Experimental quantification of contaminant ingress into a buried leaking pipe during transient events". In: *Journal of Hydraulic Engineering* 142.1, p. 04015036.
- 832
- 833 George, A. and Box, E. (2000). "Influence of the sampling interval, decision limit and autocorrelation on the average run length in CUSUM charts". In: *Journal of Applied Statistics* 27.2, pp. 177–183.
- 834
- 835 Graham, M., Chakraborti, S., and Mukherjee, A. (2014). "Design and implementation of CUSUM exceedance control charts for unknown location". In: *International Journal of Production Research* 52.18, pp. 5546–5564.
- 836
- 837 Granjon, P. (2013). "The CUSUM algorithm—a small review". In:
- 838 Hamasha, M., Ali, H., and Ahmed, A. (2022). "Ultra-fine transformation of data for normality". In: *Heliyon* 8.5.
- 839 Heard, N. and Turcotte, M. (2017). "Adaptive sequential Monte Carlo for multiple changepoint analysis". In: *Journal of Computational and Graphical Statistics* 26.2, pp. 414–423.
- 840
- 841 Higham, N. (2009). "Cholesky factorization". In: *Wiley interdisciplinary reviews: computational statistics* 1.2, pp. 251–254.

- 842 Javed, A. et al. (2024). "Designing Bayesian paradigm-based CUSUM scheme for monitoring shape parameter of the Inverse Gaussian  
843 distribution". In: *Computers & Industrial Engineering* 192, p. 110235.
- 844 Jones, M. and Steiner, S. (2012). "Assessing the effect of estimation error on risk-adjusted CUSUM chart performance". In: *International  
845 journal for quality in health care* 24.2, pp. 176–181.
- 846 Jones-Farmer, L., Jordan, V., and Champ, C. (2009). "Distribution-free phase I control charts for subgroup location". In: *Journal of  
847 Quality Technology* 41.3, pp. 304–316.
- 848 Jung, D., Kang, D., et al. (2015). "Improving the rapidity of responses to pipe burst in water distribution systems: A comparison of  
849 statistical process control methods". In: *Journal of Hydroinformatics* 17.2, pp. 307–328.
- 850 Jung, D. and Lansey, K. (2015). "Water distribution system burst detection using a nonlinear Kalman filter". In: *Journal of Water  
851 Resources Planning and Management* 141.5, p. 04014070.
- 852 Kim, Y. et al. (2016). "Robust leak detection and its localization using interval estimation for water distribution network". In: *Computers  
853 & Chemical Engineering* 92, pp. 1–17.
- 854 Knoth, S. (2021). "Steady-state average run length(s): Methodology, formulas, and numerics". In: *Sequential Analysis* 40.3, pp. 405–426.
- 855 LeChevallier, M. et al. (2003). "The potential for health risks from intrusion of contaminants into the distribution system from pressure  
856 transients". In: *Journal of water and health* 1.1, pp. 3–14.
- 857 Lever, J. (2016). "Classification evaluation: It is important to understand both what a classification metric expresses and what it hides".  
858 In: *Nature methods* 13.8, pp. 603–605.
- 859 Li, J. (2021). "Nonparametric adaptive CUSUM chart for detecting arbitrary distributional changes". In: *Journal of Quality Technology*  
860 53.2, pp. 154–172.
- 861 Li, W. and Qiu, P. (2020). "A general charting scheme for monitoring serially correlated data with short-memory dependence and  
862 nonparametric distributions". In: *IIE Transactions* 52.1, pp. 61–74.
- 863 Liemberger, R. and Marin, P. (2006). "The challenge of reducing non-revenue water in developing countries—how the private sector can  
864 help: A look at performance-based service contracting". In.
- 865 Liemberger, R. and Wyatt, A. (2019). "Quantifying the global non-revenue water problem". In: *Water Supply* 19.3, pp. 831–837.
- 866 Lim, J. and Lee, S. (2024). "Efficient ARL estimation for general control charts using censored run lengths". In: *Quality Engineering*,  
867 pp. 1–10.
- 868 Liu, L., Tsung, F., and Zhang, J. (2014). "Adaptive nonparametric CUSUM scheme for detecting unknown shifts in location". In:  
869 *International Journal of Production Research* 52.6, pp. 1592–1606.
- 870 Loureiro, D. et al. (2016). "Water distribution systems flow monitoring and anomalous event detection: A practical approach". In: *Urban  
871 Water Journal* 13.3, pp. 242–252.
- 872 Lu, S. (2017). "Novel design of composite generally weighted moving average and cumulative sum charts". In: *Quality and Reliability  
873 Engineering International* 33.8, pp. 2397–2408.
- 874 Mabude, K. et al. (2021). "Generally weighted moving average monitoring schemes: Overview and perspectives". In: *Quality and  
875 Reliability Engineering International* 37.2, pp. 409–432.
- 876 Massey, F. (1951). "The Kolmogorov-Smirnov test for goodness of fit". In: *Journal of the American statistical Association* 46.253,  
877 pp. 68–78.
- 878 Misiunas, D. et al. (2006). "Failure monitoring in water distribution networks". In: *Water science and technology* 53.4–5, pp. 503–511.
- 879 Montgomery, D. (2019). *Introduction to statistical quality control*. John Wiley & Sons.
- 880 Mounce, S. and Machell, J. (2006). "Burst detection using hydraulic data from water distribution systems with artificial neural networks".  
881 In: *Urban Water Journal* 3.1, pp. 21–31.
- 882 Moustakides, G. (1986). "Optimal stopping times for detecting changes in distributions". In: *the Annals of Statistics* 14.4, pp. 1379–1387.
- 883 Nazir, H. et al. (2013). "Robust CUSUM control charting". In: *Quality Engineering* 25.3, pp. 211–224.

- 884 Nimri, W. et al. (2023). "Data-driven approaches and model-based methods for detecting and locating leaks in water distribution systems:  
885 a literature review". In: *Neural Computing and Applications* 35.16, pp. 11611–11623.
- 886 Page, E. (1954). "Continuous inspection schemes". In: *Biometrika* 41.1/2, pp. 100–115.
- 887 Palau, C., Arregui, F., and Carlos, M. (2012). "Burst detection in water networks using principal component analysis". In: *Journal of  
888 Water Resources Planning and Management* 138.1, pp. 47–54.
- 889 Peterson, R. (2021). "Finding Optimal Normalizing Transformations via best Normalize." In: *R Journal* 13.1.
- 890 Polunchenko, A. (2016). "A note on efficient performance evaluation of the Cumulative Sum chart and the Sequential Probability Ratio  
891 Test". In: *Applied Stochastic Models in Business and Industry* 32.5, pp. 565–573.
- 892 Puust, R. et al. (2010). "A review of methods for leakage management in pipe networks". In: *Urban Water Journal* 7.1, pp. 25–45.
- 893 Romano, M., Kapelan, Z., and Savic, D. (2014). "Automated detection of pipe bursts and other events in water distribution systems". In:  
894 *Journal of Water Resources Planning and Management* 4, pp. 457–467.
- 895 Romano, M., Woodward, K., and Kapelan, Z. (2017). "Statistical process control based system for approximate location of pipe bursts  
896 and leaks in water distribution systems". In: *Procedia Engineering* 186, pp. 236–243.
- 897 Romero-Ben, L. et al. (2023). "Leak detection and localization in water distribution networks: Review and perspective". In: *Annual  
898 Reviews in Control*.
- 899 Saleh, N. et al. (2023). "A review and critique of auxiliary information-based process monitoring methods". In: *Quality Technology &  
900 Quantitative Management* 20.1, pp. 1–20.
- 901 Shu, L., Jiang, W., and Tsui, K. (2008). "A weighted CUSUM chart for detecting patterned mean shifts". In: *Journal of Quality  
902 Technology* 40.2, pp. 194–213.
- 903 Soldevila, A., Blesa, J., et al. (2016). "Leak localization in water distribution networks using a mixed model-based/data-driven approach".  
904 In: *Control Engineering Practice* 55, pp. 162–173.
- 905 Soldevila, A., Boracchi, G., et al. (2022). "Leak detection and localization in water distribution networks by combining expert knowledge  
906 and data-driven models". In: *Neural Computing and Applications* 34.6, pp. 4759–4779.
- 907 Steffelbauer, D. et al. (2022). "Pressure-leak duality for leak detection and localization in water distribution systems". In: *Journal of  
908 Water Resources Planning and Management* 148.3, p. 04021106.
- 909 Steiner, S. et al. (2000). "Monitoring surgical performance using risk-adjusted cumulative sum charts". In: *Biostatistics* 1.4, pp. 441–452.
- 910 Tukey, J. (1977). "Exploratory data analysis". In: *Reading/Addison-Wesley*.
- 911 Vrachimis, S. et al. (2022). "Battle of the leakage detection and isolation methods". In: *Journal of Water Resources Planning and  
912 Management* 148.12, p. 04022068.
- 913 Wald, A. (1945). "Sequential Tests of Statistical Hypotheses". In: *The Annals of Mathematical Statistics* 16.2, pp. 117–186.
- 914 Wan, X. et al. (2022). "Literature review of data analytics for leak detection in water distribution networks: A focus on pressure and flow  
915 smart sensors". In: *Journal of Water Resources Planning and Management* 148.10, p. 03122002.
- 916 Wang, X. et al. (2020). "Burst detection in district metering areas using deep learning method". In: *Journal of Water Resources Planning  
917 and Management* 146.6, p. 04020031.
- 918 Woodall, W. and Ncube, M. (1985). "Multivariate CUSUM quality-control procedures". In: *Technometrics* 27.3, pp. 285–292.
- 919 Wu, X., Peng, S., et al. (2023). "Leakage Detection in Water Distribution Networks Based on Multi-Feature Extraction from High-  
920 Frequency Pressure Data". In: *Water* 15.6, p. 1187.
- 921 Wu, Y., Liu, S., and Kapelan, Z. (2024). "Addressing data limitations in leakage detection of water distribution systems: Data creation,  
922 data requirement reduction, and knowledge transfer". In: *Water Research*, p. 122471.
- 923 Yu, X. and Cheng, Y. (2022). "A comprehensive review and comparison of CUSUM and change-point-analysis methods to detect test  
924 speededness". In: *Multivariate Behavioral Research* 57.1, pp. 112–133.
- 925 Zhang, X. and Woodall, W. (2015). "Dynamic probability control limits for risk-adjusted Bernoulli CUSUM charts". In: *Statistics in  
926 medicine* 34.25, pp. 3336–3348.